We are IntechOpen,
the world's leading publisher of
Open Access books
Built by scientists, for scientists

4,800
Open access books available

122,000
International authors and editors

135M
Downloads

Our authors are among the

154
Countries delivered to

TOP 1%
most cited scientists

12.2%
Contributors from top 500 universities

BOOK CITATION INDEX
CLARIVATE ANALYTICS
INDEXED

WEB OF SCIENCE™

Selection of our books indexed in the Book Citation Index
in Web of Science™ Core Collection (BKCI)

Interested in publishing with us?
Contact book.department@intechopen.com

Numbers displayed above are based on latest data collected.
For more information visit www.intechopen.com

1

Magnetic Microsensors

Căruntu George and Panait Cornel
Faculty of Electronics, Electrotechnics and Computer Science,
Constanta Maritime University,Constanta,
Romania

1. Introduction

In the presence of a magnetic field, the Hall effect takes place in the active region of the transistors, however their magnetic sensitivity is insignificant.Moreover, the Hall effect may interfere with the action of a bipolar transistor in many ways which makes the analysis and optimization of devices much more difficult.

However, there are also magnetotransistors structures in which, under appropriate operating conditions the magnetic sensitivity increases to values useful in practical work. In this way integrated magnetic sensors useful for emphasizing and measuring mechanical and geometrical quantities can be obtained.

The double-collector bipolar magnetotransistors

1.1 The general characterization of the double-collector bipolar magnetotransistors

Figure 1.1 shows the cross section of a double collector *npn* vertical magnetotransistor operating on the current deflection principle [1]. This structure is compatible with the bipolar integrated circuit technology.
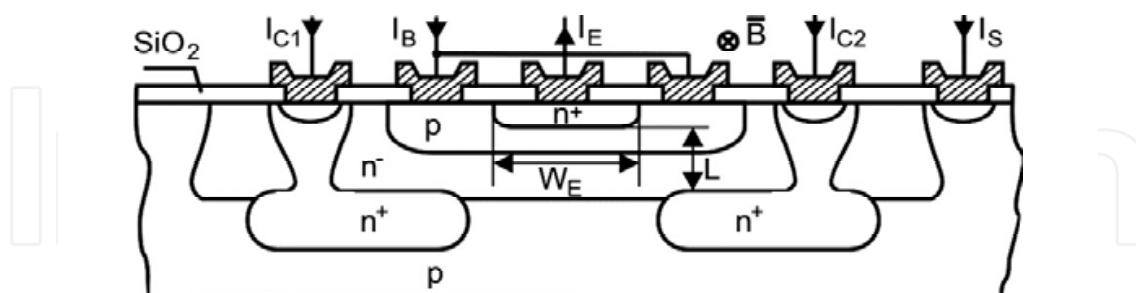

Fig. 1.1. The structure of a double-collector magnetotransistor

The most of the *n* type low-doped epitaxial layer serves as the collector region and is depleted of the charge carriers upon reverse biasing of the collector-base junction. The two collector contacts are realised by splitting the buried layer (n^+). L is the collector-emitter distance, and W_E is the width of the emitter. In the absence of the magnetic field the electron flow injected into the emitter, which crosses the base is symmetrical and the two collector currents are equal: $I_{C1} = I_{C2}$. In the presence of a magnetic field having the

induction $\bar{B}$ parallel with the device surface, the distribution of the emitter electron current becomes asymmetrical and causes an imbalance of the collector currents: $\Delta I_C = I_{C1} - I_{C2}$.

The analysed magnetotransistor operates in the Hall current mode and ΔI_C depends on the Hall transverse current. Assimilating the low-dopped epitaxial layer of the collector region with a short Hall plate, and based on the properties of dual Hall devices it results [2]:

$$\Delta I_C = \frac{I_H}{2} = \frac{1}{2}\mu_{Hn} \cdot \frac{L}{W_E} \cdot G \cdot I_C \cdot B \qquad (1.1)$$

where μ_{HCh} is the carriers Hall mobility in the channel, G denotes the geometrical correction factor and $I_C = I_{C1}(0) + I_{C2}(0)$.

1.2 The sensor response and the sensitivity related to the bias current
The sensor response is expressed by:

$$h(B) = \frac{\Delta I_C}{(I_{C1} + I_{C2})_{B=0}} = \frac{1}{2}\mu_{Hn}\frac{L}{W_E} \cdot G \cdot B_\perp \qquad (1.2)$$

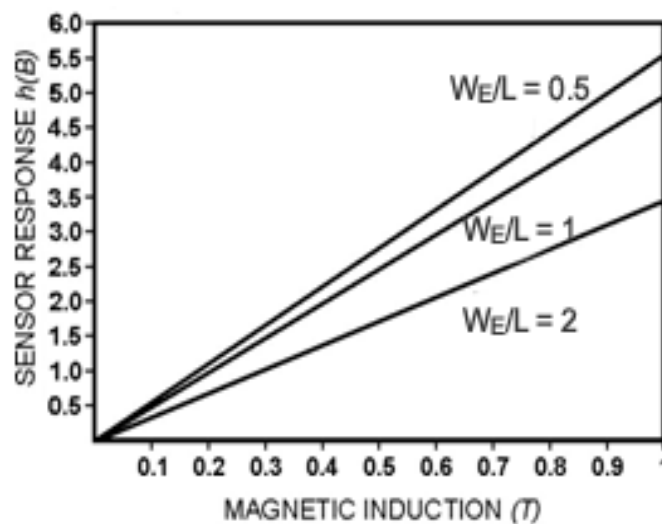and it is linear for induction values which satisfy the condition: $\mu_H^2 \cdot B_\perp^2 \ll 1$

Fig. 1.2. The $h(B)$ depending on B for three devices of different geometry

In figure 1.2 the geometry influence on h(B) values for three magnetotransistor structures can be seen ratios $W_E / L \ (W_E = 50\mu m)$.

$$\text{MGT1: } W_E / L = 0.5, \ (L / W_E)G = 0.72;$$

$$\text{MGT2: } W_E / L = 1, \ (L / W_E)G = 0.68;$$

$$\text{MGT3: } W_E / L = 2, \ (L / W_E)G = 0.46;$$

It is noticed that the response $h(B)$ is maximum for $W_E/L = 0.5$ structure. Decreasing the emitter-collector distance, $h(B)$ decreases with 37.5% for $W_E = 2L$, as compared to the maximum value. The sensor response decreases with 10.7%, comparative with $W_E/L = 0.5$ structure if the distance between emitter and collector doubles. For the same geometry $W_E/L = 0.5$, the response is depending on material features. In figure 1.3 $h(B)$ values of three sensors MGT1, MGT2, MGT3 are shown, realized on

$$\text{Si } (\mu_{H_n} = 0.15 m^2 V^{-1} s^{-1}),$$

$$\text{InP } (\mu_{H_n} = 0.46 m^2 V^{-1} s^{-1})$$

$$\text{GaAs } (\mu_{H_n} = 0.80 m^2 V^{-1} s^{-1}).$$
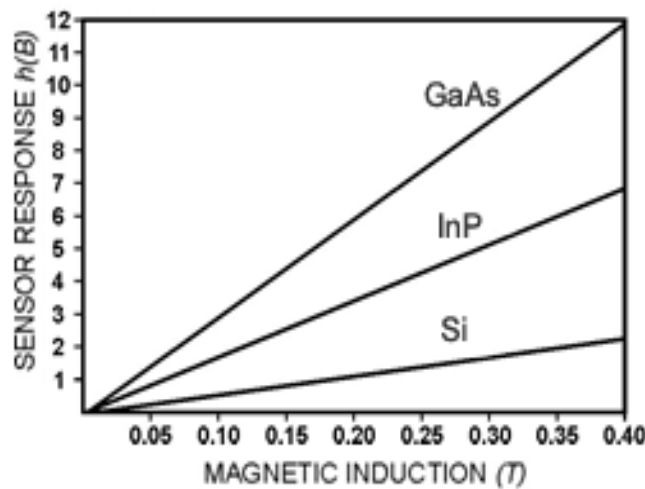

Fig. 1.3. The *h(B)* depending on *B* for three devices on different materials

A magnetotransistor may be regarded as a modulation transducer that converts the magnetic induction signal into an electric current signal.
This current signal or output signal is the variation of collector current, caused by induction $B_\perp$.
The absolute sensitivity of a magnetotransistor used as magnetic sensors is:

$$S_A = \left| \Delta I_C / B \right| = \frac{1}{2} \mu_{H_n} \cdot \frac{L}{W_E} G \cdot I_C \tag{1.3}$$

The magnetic sensitivity related to the devices current is defined as follows:

$$S_I = \frac{1}{I_C} \left| \frac{\Delta I_C}{B_\perp} \right| = \frac{1}{2} \mu_{H_n} \frac{L}{W_E} G \tag{1.4}$$

For a given induction $(B = 0,4T)$ and at given collector current $I_C = 1mA$, the sensitivity depends on the device geometry and the material properties. In table 1.1 the obtained values for five magnetotransistors structures are presented.

The analysis of the main characteristics of the double-collector magnetotransistor shows that the $W_E / L = 0.5$ structure is theoretically favourable to high performance regarding signal-to-noise ratio, as well as the offset equivalent magnetic induction. Also substituting the silicon technology by using other materials such as GaAs or InSb with high carriers mobility values assure higher characteristics of the sensors

	W_E / L	$\mu_{Hn}[m^2V^{-1}s^{-1}]$	$S_I[T^{-1}]$
MGT1	2	0,15 Si	0,035
MGT2	1	0,15 Si	0,05
MGT3	0,5	0,15 Si	0,055
MGT4	0,5	0,46 InP	0,168
MGT5	0,5	0,85 GaAs	0,292

Table 1.1. The numerical values of the supply-current-related sensitivity.

1.3 The offset equivalent magnetic induction

The difference between the two collector currents in the absence of the magnetic field is the offset collector current:

$$\Delta I_{C_{off}} = I_{C1}(0) - I_{C2}(0) \tag{1.5}$$

The causes consist of imperfections specific to the manufacturing process: the contact non-linearity, the non-uniformity of the thickness and of the epitaxial layer doping, the presence of some mechanical stresses combined with the piezo-resistive effect.

To describe the error due to the offset the magnetic induction is determined, which produces the imbalance $\Delta I_C = \Delta I_{C_{off}}$. The offset equivalent magnetic induction is expressed by considering the relation (4):

$$B_{off} = \frac{\Delta I_{C_{off}}}{S_I I_C} = \frac{2}{\mu_{Hn}} \cdot \frac{\Delta I_{C_{off}}}{I_C} \cdot \left(G \frac{L}{W_E} \right)^{-1} \tag{1.6}$$

Considering $\Delta I_{C_{off}} = 0.10\mu A$ and assuming that the low magnetic field condition is achieved, in figure 1.4 the dependence of B_{off} on I_C for three magnetotransistors with the same geometry $W_E / L = 0.5$ realised from different materials is presented:

$$\text{MGT1: Si with } \mu_{Hn} = 0.15m^2V^{-1}s^{-1} ;$$

$$\text{MGT2: InP with } \mu_{Hn} = 0.46m^2V^{-1}s^{-1} ;$$

$$\text{MGT3: GaAs with } \mu_{Hn} = 0.85m^2V^{-1}s^{-1} .$$

The geometry influence upon B_{off} is shown in figure 1.5 by simulating three magnetotransistors structures realised from silicon and having different W_E / L ratios.

$$\text{MGT1:} \quad W_E / L = 0,5; \quad GL / W_E = 0.73;$$

$$\text{MGT2:} \quad W_E / L = 1; \quad GL / W_E = 0.67;$$

$$\text{MGT3:} \quad W_E / L = 2; \quad GL / W_E = 0.46;$$

If the width of the emitter is maintained constant, B_{off} as the emitter-collector distance decreases. This kind of minimum values for the offset equivalent induction are obtained with the device which has $L = 2W_E$, and in the MGT3 device these values are 53.5% bigger.
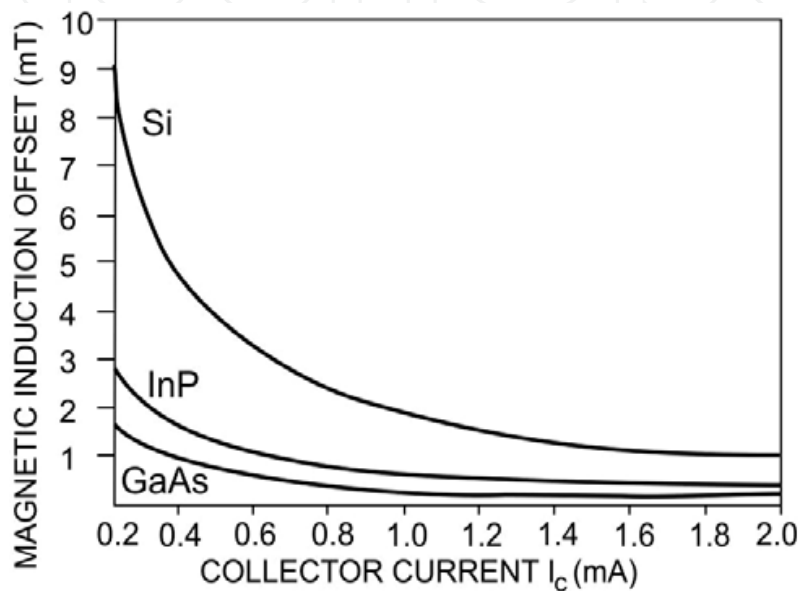

Fig. 1.4. The B_{off} depending on the collector current IC for three devices of different materials
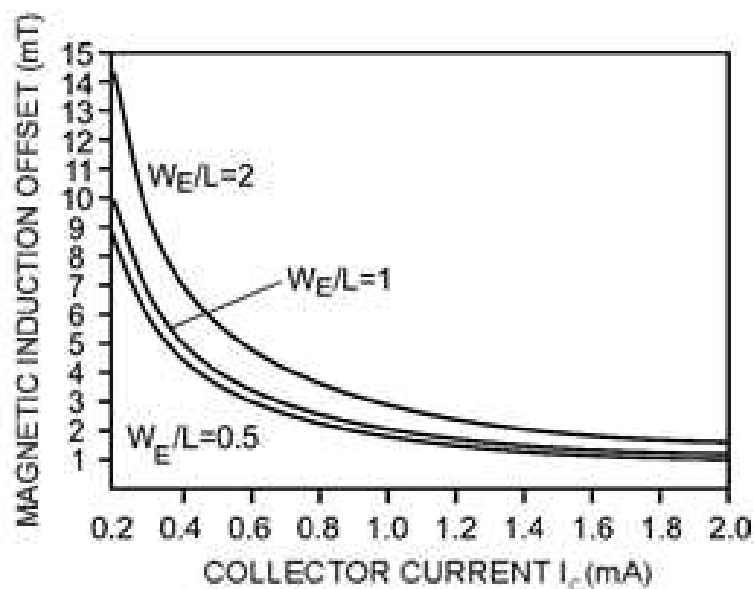
Fig. 1.5. The B_{off} depending on the collector current I_C for three devices of different geometry

1.4 Signal-to-noise ratio

The noise affecting the collector current of a magnetotransistor is shot noise and 1/f noise. Signal-to-noise ratio is defined by:

$$SNR(f) = \frac{\Delta I_C}{[S_{NI}(f) \cdot \Delta f]^{1/2}} \tag{1.7}$$

where Δf denotes a narrow frequency band around the frequency f, and $S_{NI}(f)$ denotes the noise current spectral density in the collector current.

In case of shot noise, the noise current spectral density at frequencies over 100 Hz is given by [3]:

$$S_{NI} = 2qI \tag{1.8}$$

where I is the device current.

In case of shot noise, in a narrow range f of frequency values, By substituting (1.1) and (1.8) into (1.7) it results that:

$$SNR(f) = \frac{1}{2\sqrt{2}} \mu_{Hn} (\frac{L}{W_E} G) \frac{I_C}{(q \cdot I \cdot \Delta f)^{1/2}} B_\perp \ge \frac{1}{2\sqrt{2}} \mu_{Hn} (\frac{L}{W_E} G) \frac{I_C^{1/2}}{(q\Delta f)^{1/2}} B_\perp \tag{1.9}$$

To emphasise the dependence of $SNR(f)$ on the device geometry there (figure 1.6) three magnetotrasistor structure realised on silicon ($\mu_{Hn} = 0.15 m^2 V^{-1} s^{-1}$)were simulated having different rations W_E / L ($W_E = 40\mu m$; $\Delta f = 1$; $I_C = 1mA$).

$$MGT1: W_E / L = 2 ;$$

$$MGT2: W_E / L = 1 ;$$
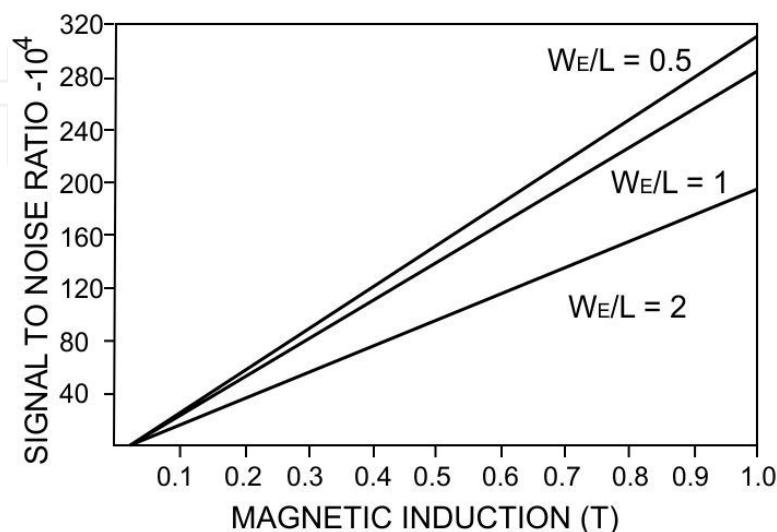
$$MGT3: W_E / L = 0.5 ;$$

Fig. 1.6. *SNR(f)* depending on *B* for three devices of different geometry

The device were biased in the linear region at the collector current $I_C = 1mA$, the magnetic field has a low level ($\mu_H^2 B^2 << 1$).

It is noticed that the $SNR(f)$ is maximum for $W_E / L = 0.5$ and for smaller values of this ratio. For the same B magnetic induction, increasing the emitter width, $SNR(f)$ decreases with 37.2% for $W_E = 2L$ As compared to the maximum value. In case of $1/f$ noise, the noise current spectral density at the device output is given by [4]:

$$S_{NI}(f) = I^2 \alpha N^{-1} f^{-\beta} \tag{1.10}$$

where I is the device current, $N = n\delta LW_E$ is the total number of charge carriers in the device, α is a parameter called the Hooge parameter and $\beta \cong 1 \pm 0.1$ (typically). For semiconductors, it is reported that α values range from 10^{-9} to 10^{-7}. Substituting (1.1) and (1.10) into (1.7) it is obtained:

$$SNR(f) \cong \frac{(ndLW_E)^{1/2}}{2\alpha^{1/2}} \cdot \mu_{Hn} \left(\frac{f}{\Delta f}\right)^{1/2} \cdot \left(\frac{L}{W_E}G\right) \cdot B_\perp \tag{1.11}$$

To illustrate the $SNR(f)$ dependence on device geometry three split-collector magnetotransistor structures realised on Si were simulated (figure 1.7).

MGT1: $W_E / L = 0.5$;

MGT2: $W_E / L = 1$;

MGT3: $W_E / L = 2$.

It is considered that: $f = 4Hz$, $\Delta f = 1Hz$, $n = 4.5 \cdot 10^{21} m^{-3}$, $d = 4 \cdot 10^{-6} m$, $\alpha = 10^{-7}$, $q = 1.9 \cdot 10^{-6} C$, the devices being biased in the linear region and the magnetic field having a low level. For the same magnetic induction B, $SNR(f)$ is maximum in case of $L = 2W_E$. The increasing of the emitter collector distance causes the decreasing of $SNR(f)$ with 35.2% for a square structure with 69.1% for $W_E = 2L$.
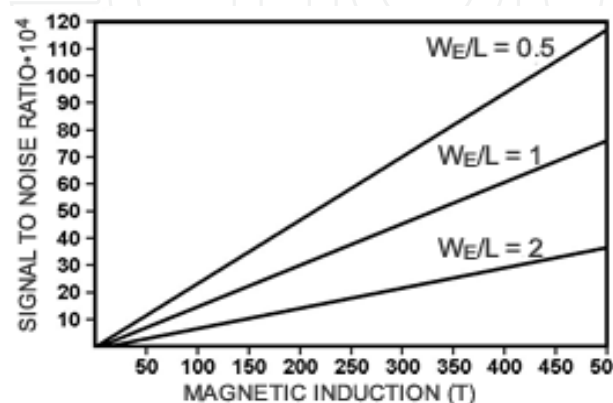

Fig. 1.7. *SNR(f)* depending on *B* for three devices of different geometry

1.5 The detection limit

A convenient way of describing the noise properties of a sensor is in terms of detection limit, defined as the value of the measurand corresponding to a unitary signal-to-noise ratio.
In case of shot noise, for double-drain magnetotransistors using (1.9) it results for detection limit it results that:

$$B_{DL} \leq \frac{2\sqrt{2}\left(q\Delta f\right)^{1/2}}{\mu_{Hn}\left(L/W_E\right)G}I_C^{-1/2} \tag{1.12}$$

To illustrate the B_{DL} dependence on device geometry (figure 1.8) three double-collector magnetotransistor structures on silicon $\left(\mu_{Hn} = 0.15 m^2 V^{-1} s^{-1}\right)$ were simulated having

MGT1: $W_E/L = 0.5$;

MGT2: $W_E/L = 1$;

MGT3: $W_E/L = 2$;
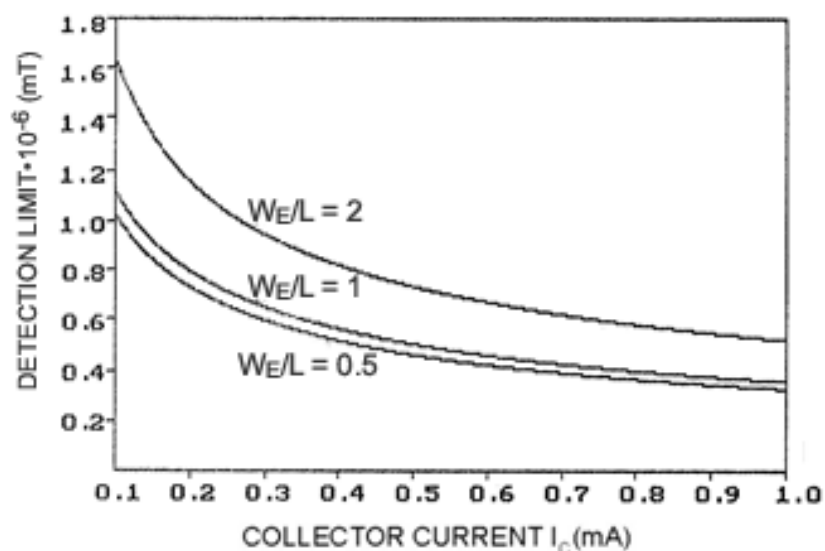
Fig. 1.8. B_{DL} depending on the collector total current for three devices of different geometry

It is noticed that the B_{DL} is minimum for $W_E/L = 0.5$ structure. For optimal structure B_{DL} decreases at materials of high carriers mobility.
In figure 1.9 the material influence on B_{DL} values for three double-collector magnetotransistor structures realised from *Si*, *GaSb* and *GaAs* can be seen having the same size: $L = 200 \mu m$, $W_E = 100 \mu m$.

MGT1: *Si* with $\mu_{Hn} = 0,15 m^2 V^{-1} s^{-1}$;

MGT2: GaSb with $\mu_{Hn} = 0,5 m^2 V^{-1} s^{-1}$;

MGT3: *GaAs* with $\mu_{Hn} = 0,8 m^2 V^{-1} s^{-1}$.

By comparing the results for the two types of Hall devices used as magnetic sensors a lower detection limit of almost 2-order in double-colletor magnetotransistors is recorded.
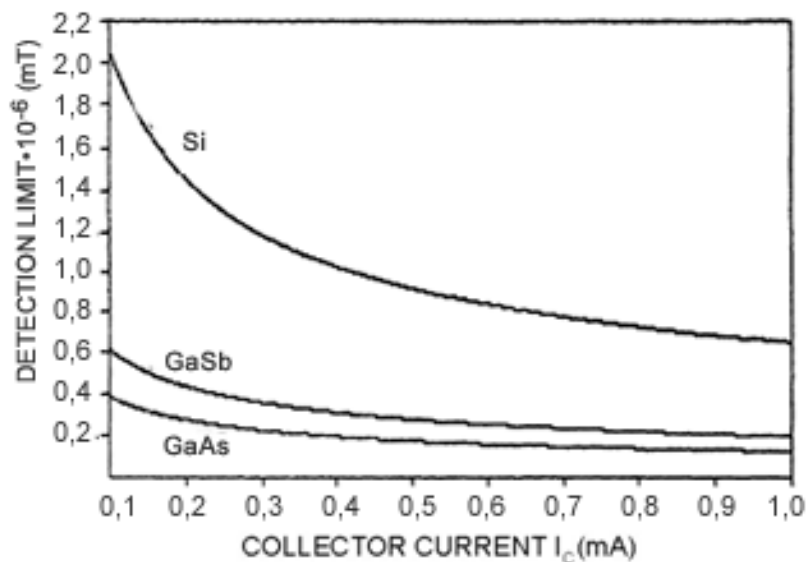

Fig. 1.9. B$_{DL}$ depending on the drain current for three devices of different materials

1.6 The noise-equivalent magnetic induction

The noise current at the output of a magnetotransistor can be interpreted as a result of noise equivalent magnetic induction.
The mean square value of noise magnetic induction (NEMI) is defined by:

$$\left\langle B_N^2 \right\rangle = (\int_{f1}^{f2} S_{NI}(f) \cdot df)(S_I \cdot I_C)^{-2}$$ (1.13)

In case of shot noise, by substituting (1.1) and (1.8) into (1.13) it results that:

$$< B_N^2 > = 2qI \cdot \Delta f \cdot 4\left(\frac{W_E}{L}\right)^2 \cdot \frac{1}{G^2 \mu_{Hn}^2} \cdot \frac{1}{I_C^2} \le$$
$$\le 8q\left(\frac{W_E}{L}\right)^2 \cdot \frac{\Delta f}{G^2} \cdot \frac{1}{\mu_{Hn}^2} \cdot \frac{1}{I_C}$$ (1.14)

Considering the condition of low value magnetic field fulfilled ($\mu_H^2 B^2 << 1$),a maximum value for $(L/W_E)G = 0.74$, if $W_E/L < 0.5$. [5] is obtained
In this case:

$$< B_N^2 >_{min} \le 14.6q \frac{\Delta f}{I_C} \cdot \frac{1}{\mu_{Hn}^2}$$ (1.15)

In figure 1.10 NEMI values obtained by simulation of three magnetotransistors structures from different materials are shownMGT_1: Si with $\mu_{Hn} = 0.15 m^2 V^{-1} s^{-1}$

$$MGT_2: \text{InP with } \mu_{Hn} = 0.46 m^2 V^{-1} s^{-1}$$

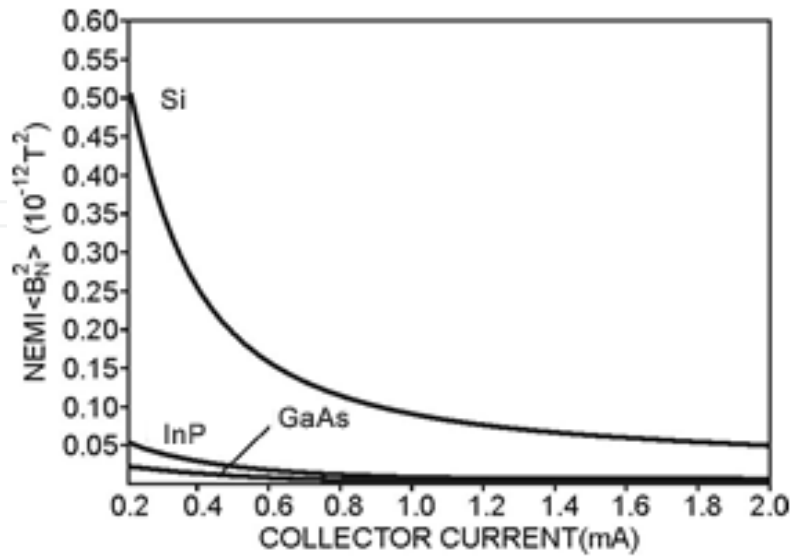MGT_3: GaAs with $\mu_{Hn} = 0.85 m^2 V^{-1} s^{-1}$

Fig. 1.10. NEMI depending on the collector current for three devices of different materials

To emphasize the dependence of NEMI on device geometry (figure 1.11) three double-collector magnetotransistors structures realised on silicon, $\mu_{Hn} = 0.15 m^2 V^{-1} s^{-1}$ were simulated, having different ratios W_E/L $\left(W_E = 50 \mu m\right)$. The devices were based
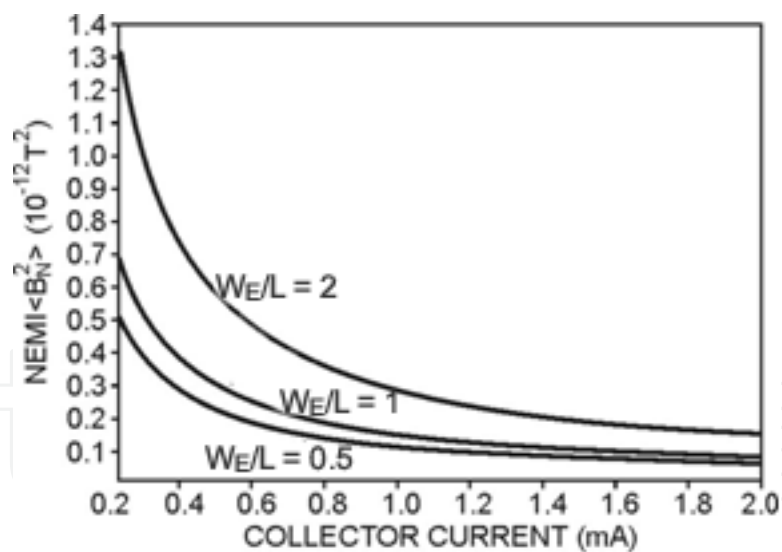

Fig. 1.11. NEMI depending on the collector current for three devices of different geometry

MGT_1 with $W_E/L = 0.5$ and $\left(LG/W_E\right)^2 = 0.576$

MGT_2 with $W_E/L = 1.0$ and $\left(LG/W_E\right)^2 = 0.409$

MGT_3 with $W_E/L = 02$ and $\left(LG/W_E\right)^2 = 0.212$

It is noticed that the NEMI is minimum for $W_E/L = 0.5$, and for smaller values of this ratio. The decreasing of the channel length causes the increase of NEMI with 40.8 % for a square structure $W_E = L$ and with 173 % for $W = 2L$.

Conclusions

The magnetotransistors have a lower magnetic sensitivity than the conventional Hall devices but allow very large signal-to-noise ratios, resulting in a high magnetic induction resolution. The analysis of the characteristics of two magnetotreansistors structures shows that the $W/L = 0.5$ ratio is theoretically favourable to high performance regarding signal-to-noise ratio, as well as the noise equivalent magnetic induction

Also substituting the silicon technology by using other materials such as GaAs or InSb with high carriers mobility values assure higher characteristics of the sensors

The uses of magnetotransistors as magnetic sensors allows for the achieving of some current-voltage conversion circuits, more efficient that conventional circuits with Hall plates.

The transducers with integrated microsensors have a high efficiency and the possibilities of using them ca be extended to some measuring systems of thickness, short distance movement, level, pressure, linear and revolution speeds.

1.7 System to monitor rolling and pitching angles

The efficient operation of the modern maritime ships requires the existence of some reliable command, watch and protection systems that permit transmission, processing and receiving of signals with great speed and reduced errors.

On most of the merchant ships the watch of the rolling and the pitching is done by conventional instruments as gravitational pendulum. The indication of the specific parameters is continuous, the adjustment operations are manual and the transmissions of the information obtained in the measurement process, at distance is not possible.

An automatic and efficient surveillance system ensures the permanent indication of the inclination degree of the ship , the optic and the sound warning in case of exceeding the maximum admissible angle and the simple transmission of the information at distance.

1.7.1 Installation for the measurement of the rolling and pitching thatuses magnetotransistors

The presentation of the transducers

The primary piece of information about the rolling and pitching angle is obtained with the help of the classical system used on ships, with the difference that at the free end of the pendulum,a permanent magnet with reduced dimensions is fixed provided with polar parts shaped like those used in the construction of the magnetoelectric measurement devices. Along the circle arc described by the free end of the pendulum , there are disposed at equal lengths, accordingly to the displacements of 1° for the rolling and of 1° 30′ for the pitching, twenty magnetotransistors, ten on one side and ten on the other side of the equilibrium position.

Due to the high inertia moment, the pendulum maintains its vertical position, and actually during the rolling and pitching the graded scale, fixed on the wall, is the one that moves at the same time with the ship.

The transducer for the indication of the rolling is disposed in a vertical plane, transverse on the longitudinal axis of the ship, and the one for the pitching in a vertical plane that contains or is parallel with the longitudinal axis of the ship. In order to simplify the presentation will consider that the pendulum is the one that moves in with the graded scale. In figure 1.14 the principle diagram of the transducer is shown vertical bipolar magnetotransistor with double collector. In the absence of the magnetic field, the two collector currents are equal and the output of the comparator is in "DOWN" state (logical level „0"). In the presence of a field of induction B, parallel with the device surface, a lack of poise between the two collector currents ΔI_C is produced and at the input of comparator is applied the voltage:

$$\Delta V_C = \mu_H \left(L / W_E \right) G R_C I_C B \tag{1.18}$$
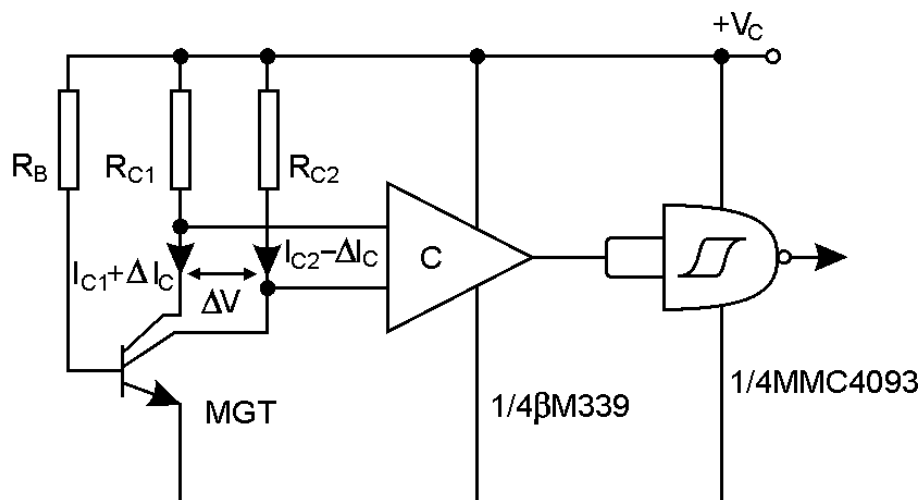

Fig. 1.14. The electric diagram of transducer

This voltage is applied to a comparator with hysteresis, which acts as a commutator. The existence of the two travel thresholds ensure the immunity of the circuit at noise monostable made with *MMC 4093* ensures the same duration for the transducers generated pulses. Applied to the comparator *C*, this voltage changes its state and the output goes on logical level "1".

The principle block diagram. The description of working

When the ship lists, the permanent magnet of the pendulum will scavenge in turn a number of magnetotransistors, and the signals from their outputs will determine the tipping of the comparators. We will thus obtain impulses which are applied through an "OR" circuit at the CBM input (figure 1.15). This commands the block for the interruption of the power supply (IPS), achieving the cancellation of the potentials in the thyristors anode for a time interval of milliseconds.

At the same time the impulses generated by the transducers are transmitted with the help of separator B1, B2, …, B10 on the thyristors gates, determining their damping. Once the thyristors are damped, they maintain that state, therefore these are memorizing the last indicated value, until the power supply is cancelled. So if the rolling or the pitching have intermediate values ranging between the successive marks of the graded scale , the last complete measured value remains displayed.

For a rolling value noted with "K" , all the displays from one to "K" will work in "bright point" mode, when for the same "K" value of the rolling will be lighted, therefore the scheme allows the analogical display in bar mode.

Eliminating the diodes D1, D2, …, D9, the display will be in "bright spot" mode when for the same value "K" of rolling only the "K" display is lighted.

If the inclination of the ship reaches a limit value L settled beforehand with the help of the „K" switch , then the output signal X_L (L=1,2,…,10) commands the bistable of T type which commutes, releasing the sound alarm device.
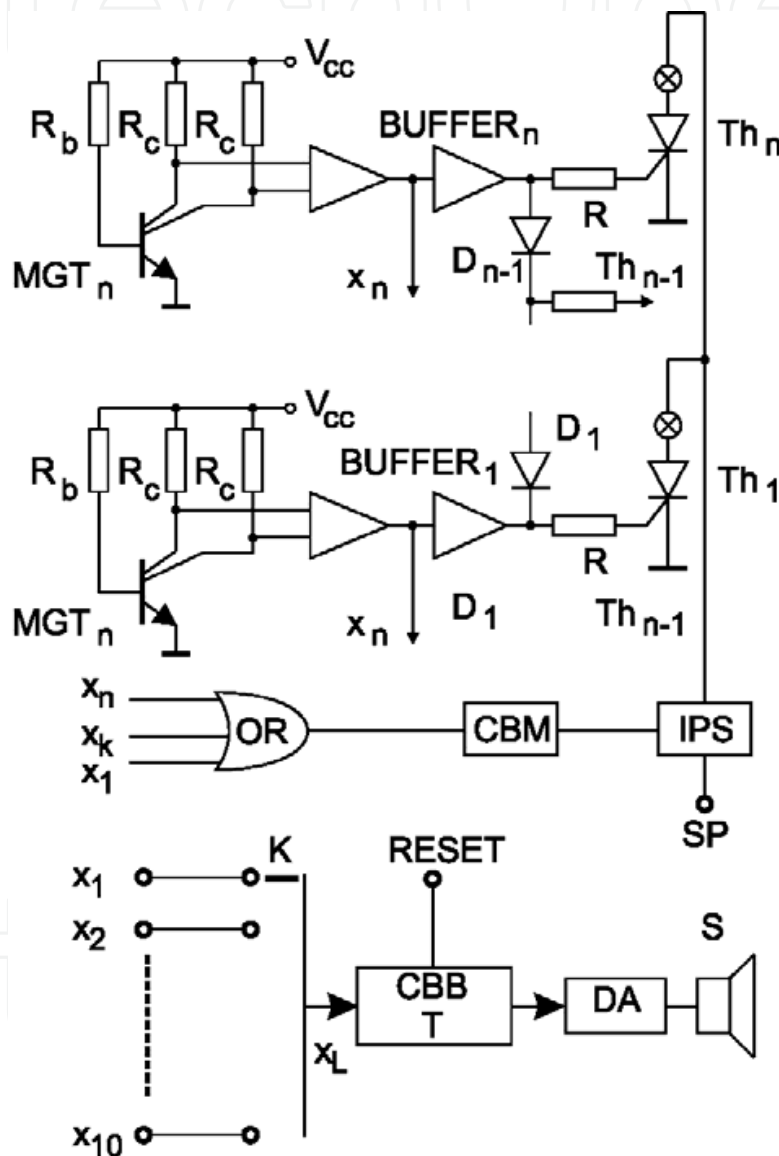
Fig. 1.15. The diagram of the installation for the measurement of the rolling and pitching

Supposing that the angle of the ship's list increases, the pendulum overtakes the „L'' position and after it touches a maximum deviation it starts the return run in which it will pass again through the front of the magneto transistor. The impulse generated by this, will swing again the bistable and the sound alarm ceases.

An undesirable situation appears when the maximum inclination of the ship has precisely the pre-established "L" value or it exceeds very little this value. In this case, in the return

run of the pendulum a new "X_L" impulse, which will swing again the bistable, is no longer generated and therefore the acoustic alarm is maintained although the inclination angle has been reduced.

This drawback can be eliminated either by using the "X_{L-1}" output for the bistable command on the input or by replacing the bistable with one of R-S or J-K type commanded by "X_L" and "X_{L-1}" signals. The "X_L" signal establishes the placing in function of the alarming device and the X_{L-1}" signal the blockage of this device, which permits to obtain a safety hysteresis.

If in the scheme in figure 1.15 the diodes D1, D2, …, D9 are eliminated, then in every moment a single thyristor will be in conduction, suitable at a certain angle.

The signals in the anodes of the other blocked thyristors will be at the logical level "1" and only in the anode of the commanded thyristor the signal will have the logical level "0". This signals are applied to a binary-decimal circuit, at the output of which is obtained the value of the angle in the binary code. A decoder seven segments which commands a display with seven segments and permits the digital display of the measured value.(figure 1.16).

The binary-decimal coder can be a matrix of diodes, a matrix of connected gates in a suitable way, or a specialized circuit like those used in numerical keyboards.
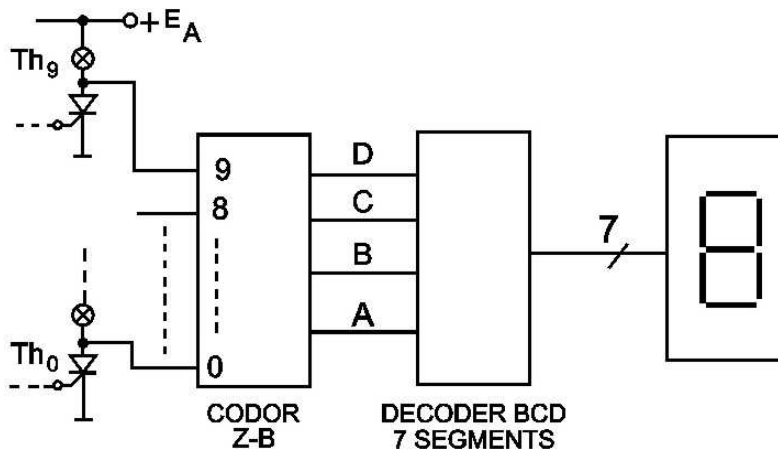

Fig. 1.16. The electrical diagram of the digital display

1.7.2 Installation for the measurement of the rolling and the pitching *that uses phototransistors*

The presentation of the transducer

The principle scheme of the photoelectric transducer is shown in figure 1.17. Classical system on board ships,is used but at the free end of the gravitational pendulum an electroluminiscent diode (LED) in visible or in infrared is set moves along an arc of circle on which the phototransistors are placed. The LED pendulum and the phototransistors are fixed in a box which protects them from the exterior light.

The power supply is ensured from a stabilized source of 12V.

Through one phototransistor, with off–load base / unconnected base and in the absence of the light the   so-called "dark current" will flow between the emitter and the collector.

$$I_D = \beta \cdot I_{CB0} \tag{1.19}$$

where β denotes the amplification factor of the transistor and I_{CB0} is the current generated by the base-collector junction, in the absence of light.

When the base-collector junction is illuminated, through this an illumination current will appear (I_l) and this current is all the intense as the illumination is bigger, and the collector current becomes:

$$I_C = \beta\left(I_{CB0} + I_l\right) \tag{1.20}$$

Since the phototransistors are blocked in the absence of the illumination, the output voltage of the collector is practically equal with the value of the power supply $(+E)$. In the moment of the illumination the phototransistors are saturated and the collector voltage lowers to U_{CEsat} value. Therefore the signal given by the transducer is in shape of negative power impulses with the amplitude approximately equal to the value of the power supply
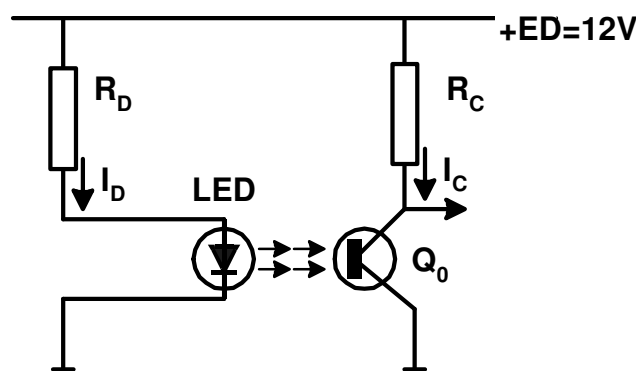
Fig. 1.17. The photoelectric transducer

The principle block diagram. The description of working

Because the measurement of the rolling and the pitching is in fact reduced to the measurement of an angle, the measurement system is made up of two identical measurement blocks, one for the rolling and the other for the pitching, with the difference that the measurement transducer will be placed differently: the one for the rolling on the transversal axis of the ship and the one for the pitching on the longitudinal ship's axis.

In figure 1.18 it is presented the block scheme of the measurement system of the inclination angle of the ship on the longitudinal (transversal) axis of the ship. In this scheme the following notations have been used: TM -measurement transducer of the rolling (pitching); CF - formatter circuit; CM-memory cell; IO - optic indicator; CR -resetting circuit; OC - commanded oscillator; AAF – audio frequency amplifier; SB - supply block; HA - warning block.

It is noticed that the measurement system is made up "2n+1" identical measurement and display chains:
- a chain corresponding to the equilibrium position (zero)
- "n" chains corresponding to „n" number of values of the port inclination angle (stern)
- "n" chains corresponding to „n" number of values of the starboard inclination angle (bow)

The measurement transducer (TM) supplies the necessary information about the inclination angle in a discrete way, meaning that the total angle can be measured has been divided into "2n" sectors ("n" port sectors "n" starboard sectors), and the transducer supplies one impulse for the output suitable for the inclination angle reached by the ship. The impulse

suitable for this angle is processed in the formatter circuit (CF) and it is applied to the corresponding memory cell (MC), in which the information about the inclination angle of the ship is kept. This information is displayed by the optic indicator (IO) corresponding the same sector, until the ship, in her movement, reaches the same inclination angle, but moving in reverse direction. The measurement transducer generates at the same output a new impulse that wipes up the information from the memory cell and at the same time the display of the optic indicator. In this way, the measurement transducer supplies two impulses for every inclination angle of the ship, except for the maximum inclination angle, which is pre-established. In case of maximum inclination, the transducer produces a single impulse that is memorized and displayed until the ship, after she reaches the maximum inclination angle in the opposite direction, returns to the equilibrium position. In the passing moment through the equilibrium position, the impulse from the CF out put wipes up, with the help of a reset circuit (CR), the information from all the memory cells and therefore from the cells corresponding to the maximum angles for the two inclination ways of the ship. From now on the working of the system is continued from the equilibrium position.
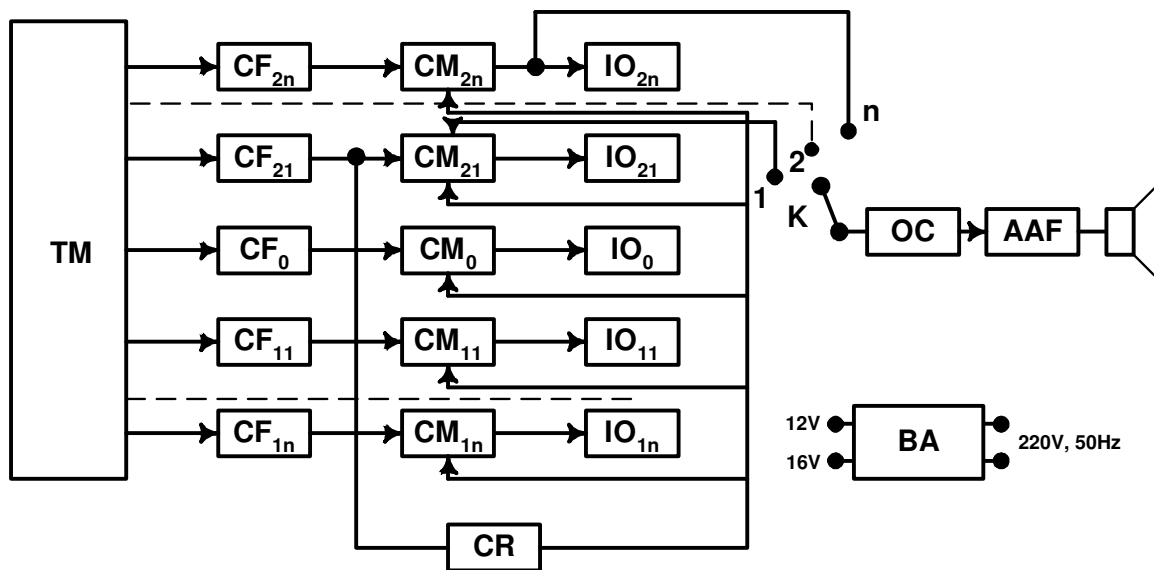
Fig. 1.18. The block diagram of the measurement system based on the phototransistors

Conclusions

The use of another transducer type for the measurement of the rolling and the pitching, namely the classic solution with the transducers in Gray code, would have reduced the number of the components. With such a transducer, using eight pairs of LED phototransistors a measurement accuracy of the angle, better with $\pm 1°$, could have been obtained. Besides, this system allows the long distance transmission of the information, but the solution would have required a sophisticated electronic part, the major difficulty being the precise construction achievement of the Gray transducer in eight bits.

The block scheme also contains a sound warning system, which is triggered at a maximum inclination angle pre-established with the help of "K" switch. Once this switch fixed on the desired position, the logical level from the output of the memory cell corresponding to the chosen angle, it will command and release the sound warning system.

This is made up of a command oscillator (OC), an audio frequency amplifier (AAF) and a warning horn (HA). The command signal of the sound warning system is taken over from the input of the optic indicator and not from its output, although it would have been easier to achieve this, out of safety operation reasons. The probability of the memory cell to go out of order is less than that of the optical indicator, moreover, if the optical indicator goes out of order that doesn't imply that the sound warning system gets inoperative.

2. Introduction

The possibility of modelling the channel depth by means of the external supply voltage and low value of area carrier density suggests the possibility of using the MOSFET channel as the active region of a Hall plate.

At the same time, the advantage of integrating on the same chip of a magnetic sensor and the signal processing circuit is outlined.

The Hall devices in MOS structure have some drawbacks: the carrier mobility in the channel is half of its value in the volume of the device; the increasing of *1/f* noise, and the instability of device surface.

The analysis made in this paper outlines the way in which the way of choosing the adequate choice device material and dimensions allows the improvement of CMOS technology sensors.

The double-drain magnetotransistor

2.1 The characterisation of the double-drain magnetotransistor

The double – drain MOS device (figure 2.1) is obtained from a MOSFET structure where its conventional drain region is replaced by two adjacent drain regions[7]. Consequently, the total channel current is shared between these two drain regions.
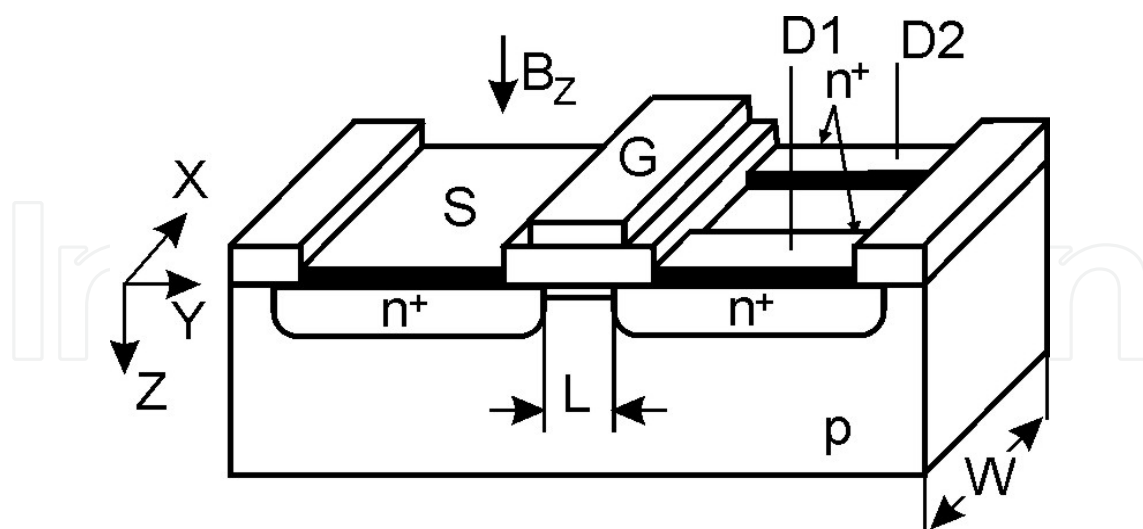
Fig. 2.1. Double-drain MOSFET magnetotransistor

The result of the bias is the linear region is the obtained of a continuous channel of approximately constant thickness, which can be assimilated with a Hall plate.

The deflection of current lines appears under the action of a magnetic field $B_\perp$, perpendicular to the device surface. The carrier deflection causes a discrepancy between two drain currents:

$$\Delta I_D = \left| I_{D1}(\overline{B}) - I_{D1}(0) \right| = \left| I_{D2}(\overline{B}) - I_{D2}(0) \right| \tag{2.1}$$

Since the output signal of the double-drain MOS magnetotransistors consists of the current variation between its terminals, this device operates in the Hall current mode. Using the features of dual Hall devices, and the Hall current expression it results [2]:

$$\Delta I_D = \frac{I_H}{2} = \frac{1}{2} \mu_{HCh} \cdot \frac{L}{W} \cdot G \cdot I_D \cdot B_\perp \tag{2.2}$$

The supply-current-related sensitivity of the devices is defined by:

$$S_I = \frac{1}{I_D} \cdot \left| \frac{\Delta I_D}{B_\perp} \right| = \frac{1}{2} \mu_{HCh} \cdot \frac{L}{W} G \tag{2.3}$$

where G denotes the geometrical correction factor and μ_{HCh} is the Hall mobility of the carriers in the channel.

For a given induction $(B = 0,4T)$ and at given drain current $I_D = 1mA$, the sensitivity depends of the device geometry and the material properties.

In table 2.1 the values for five magnetotransistors structures are presented.

Device	W/L		$S_I[T^{-1}]$
MGT1	2	0,07 Si	0,018
MGT2	1	0,07 Si	0,025
MGT3	0,5	0,07 Si	0,028
MGT4	0,5	0,23 InP	0,084
MGT5	0,5	0,42 GaAs	0,146

Table 2.1. The numerical values of the supply-current sensitivity

2.2 The sensor response

The sensor response is expressed by:

$$h(B) = \frac{\Delta I_D}{(I_{d1} + I_{D2})_{B=0}} = \frac{1}{2} \mu_{HCh} \ \frac{L}{W} \cdot G \cdot B_\perp \tag{2.4}$$

and it is linear for induction values which satisfy the condition: $\mu_H^2 \cdot B_\perp^2 \ll 1$.

In figure 2.2 the geometry influence on $h(B)$ values for three magnetotransistor structures can be seen, realised on silicon ($\mu_{HCh} = 0.07 m^2 V^{-1} s^{-1}$) and having different ratios W / L

$$\text{MGT1: } W / L = 0.5, \ (L / W)G = 0.72;$$

$$\text{MGT2: } W / L = 1, \ (L / W)G = 0.68;$$

$$\text{MGT3: } W/L = 2, \ (L/W)G = 0.46;$$

It is noticed that the response $h(B)$ is maximum for $W/L = 0.5$ structure.

For the same geometry $W/L = 0.5$, the response depends on the material features.

Decreasing the channel length, $h(B)$ decreases with 37.5% for $W = 2L$, As compared to the maximum value.

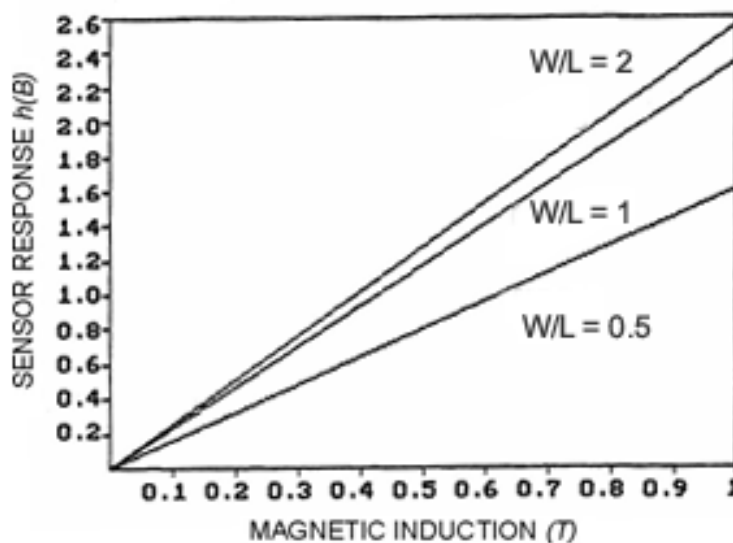The sensor response decreases with 10.7%, comparative with $W/L = 0.5$ structure if the channel length doubles.

Fig. 2.2. The *h(B)* depending on *B* for three devices of different geometry.

In figure 2.3 are shown $h(B)$ the values of three sensors MGT1, MGT2, MGT3 realised on:
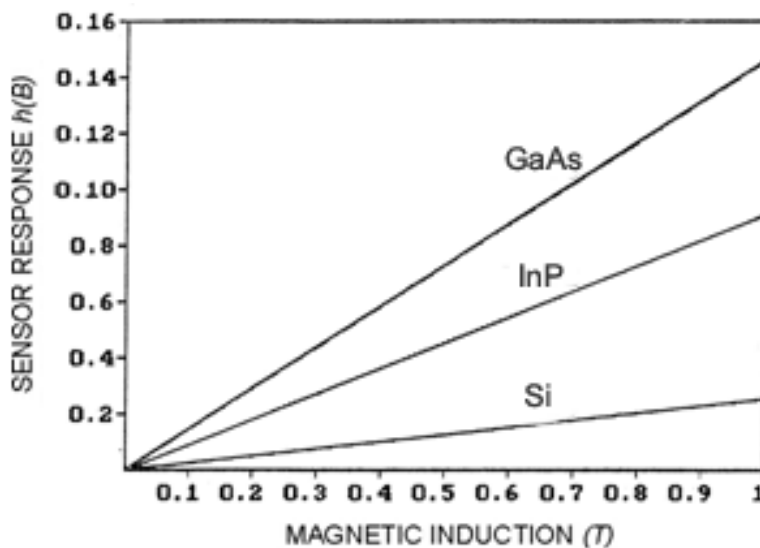
Fig. 2.3. The *h(B)* depending on *B* for three devices on different materials.

$$\text{Si}(\mu_{H_n} = 0.07 m^2 V^{-1} s^{-1});$$

$$\text{InP}(\ \mu_{H_n} = 0.23 m^2 V^{-1} s^{-1}\ );$$

$$\text{GaAs}(\ \mu_{H_n} = 0.40 m^2 V^{-1} s^{-1}\ ).$$

2.3 The offset equivalent magnetic induction

The difference between the two drain currents in the absence of the magnetic field is the offset collector current:

$$\Delta I_{D_{off}} = I_{D1}(0) - I_{D2}(0) \tag{2.5}$$

The main causes of the offset in the case of Hall devices realised in the MOS integrated circuits technology consists of imperfections specific to the manufacturing process: the misalignment of contacts, the non-uniformity of both the material and channel depth, the presence of some mechanical stresses combined with the piezo-effect.

To describe the error due to the offset the magnetic induction, which produce the imbalance $\Delta I_D = \Delta I D_{off}$ is determined..

The offset equivalent magnetic induction is expressed by considering the relation (2.3):

$$B_{off} = \frac{\Delta I_{D_{off}}}{S_I I_D} = \frac{2}{\mu_{Hn}} \cdot \frac{\Delta I_{D_{off}}}{I_D} \cdot \left(G \frac{L}{W_E} \right)^{-1} \tag{2.6}$$

Considering $\Delta I_{D_{off}} = 0.10 \mu A$ and assuming that the low magnetic field condition is achieved in figure 2.4 is presented the dependence of B_{off} on I_D for three magnetotransistors with the same geometry $W/L = 0.5$ realised from different materials:
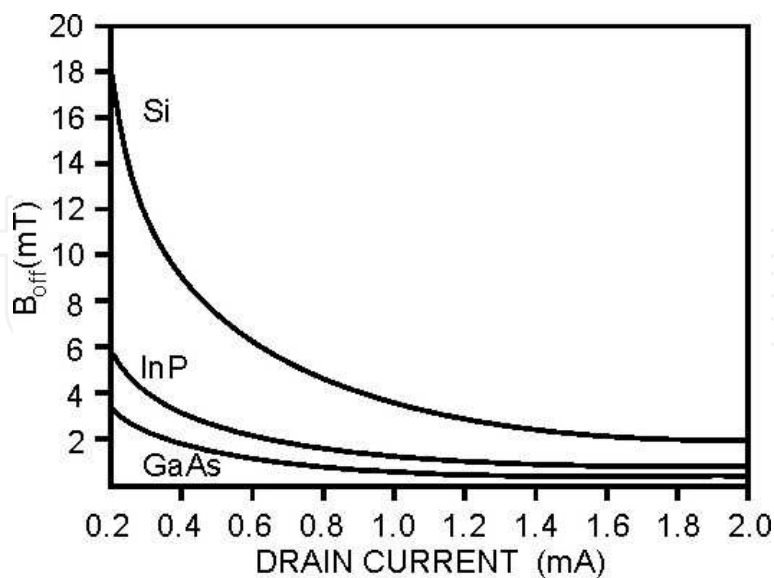
Fig. 2.4. The B_{off} depending on the drain current I_D for three devices of different materials.

$$\text{MGT1: Si,}\ \mu_{H_{Ch}} = 0.07 m^2 V^{-1} s^{-1}\ ;$$

$$\text{MGT2: InP, } \mu_{HCh} = 0.23 m^2 V^{-1} s^{-1} \text{ ;}$$

$$\text{MGT3: GaAs, } \mu_{HCh} = 0.43 m^2 V^{-1} s^{-1} \text{ .}$$

The geometry influence upon B_{off} is shown in figure 5 by simulating three magnetotransistors structures realised from silicon and having different $\dfrac{W}{L}$ ratios.

$$\text{MDD1: } \frac{W}{L} = 0,5; \quad G\frac{L}{W} = 0.73;$$

$$\text{MDD2: } \frac{W}{L} = 1; \quad G\frac{L}{W} = 0.67;$$

$$\text{MDD3: } \frac{W}{L} = 2; \quad G\frac{L}{W} = 0.46;$$

If the width of the channel is maintained constant, B_{off} increases as the channel length decreases. So that minimum values for the offset equivalent induction are obtained with the device which has $L = 2W$, and in the MDD3 device these values are 53.5% higher.
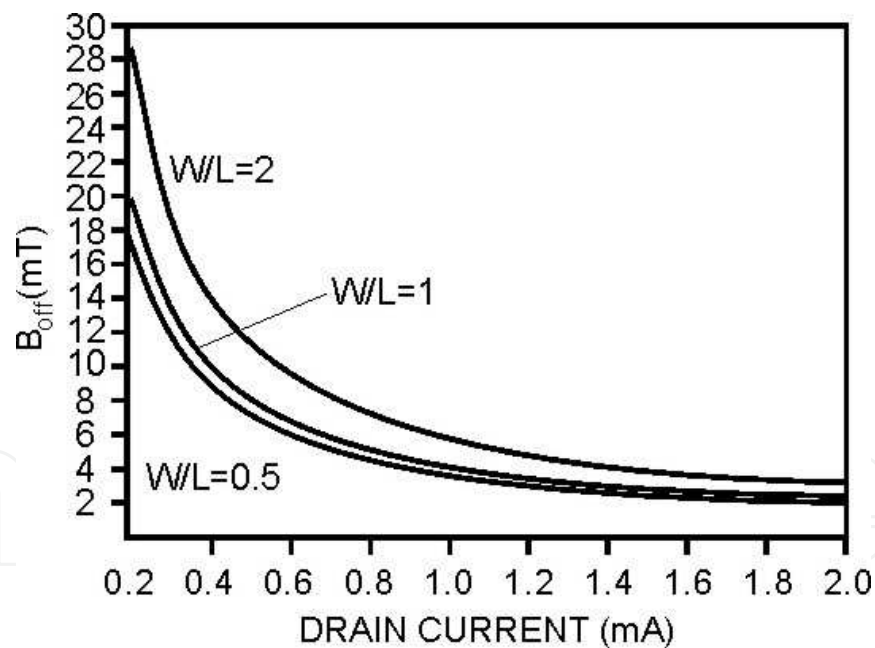
Fig. 2.5. The B_{off} depending on the drain current I_D for three devices of different geometry.

2.4 Signal – to – noise ratio

The noise affecting the drain current of a MOSFET magnetotransistors is shot noise and $1/f$ noise. Signal-to-noise is defined by [8]:

$$SNR(f) = \Delta I_D \cdot \left[S_{NI}(f) \cdot \Delta f \right]^{-1/2} \tag{2.7}$$

where Δf denotes a narrow frequency band around the frequency f, and $S_{NI}(f)$ is the noise current spectral density in the drain current. In case of shot noise by substituting (2.2) and (1.8) into (2.7) it results:

$$SNR(f) = \frac{1}{2\sqrt{2}} \mu_{HCh} \left(\frac{L}{W} G \right) \frac{I_D}{(q \cdot I \cdot \Delta f)^{1/2}} B_\perp \geq \frac{1}{2\sqrt{2}} \mu_{HCh} \left(\frac{L}{W} G \right) \frac{I_0^{1/2}}{(q\Delta f)^{1/2}} \cdot B_L \qquad (2.8)$$

In figure 2.6 is shown the *SNR(f)* dependence on magnetic induction of three MOS magnetotransistors structures of different materials ($W/L = 0.5$, $\Delta f = 1Hz$, $I_D = 1mA$)
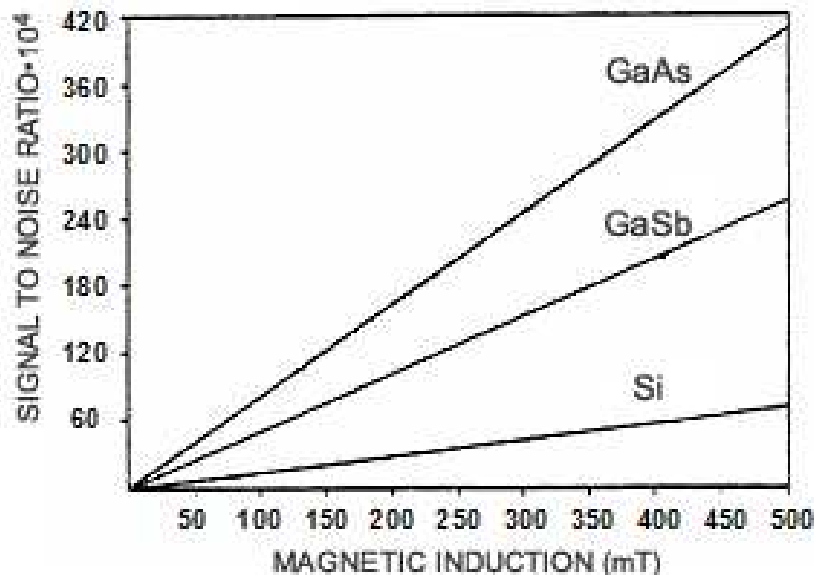
Fig. 2.6. SNR(f) depending on B for three devices of different materials.

$$MGT1{:}Si, \ \mu_{HCh} = 0.07 m^2 V^{-1} s^{-1}$$

$$MGT2{:}GaSb, \mu_{HCh} = 0.25 m^2 V^{-1} s^{-1}$$

$$MGT3{:}GaAs, \mu_{HCh} = 0.04 m^2 V^{-1} s^{-1}$$

A high value of carrier mobility causes the increasing of *SNR(f)*. So for $B = 0,5T$, *SNR(f)* increase with 60% for GaAs comparative with GaSb.

To emphasize the dependence *SNR(f)* on device geometry there (Fig. 2.7) three MOS magnetotransistors structures realised on silicon $\mu_{HCh} = 0.07 m^2 V^{-1} s^{-1}$ were simulated having different ratios L/W . ($W = 50\mu m$ $\Delta f = 1Hz$, $B = 0.2T$, $I_D = 1mA$).

$$MGT1{:} \frac{W}{L} = 2 \ \text{ and } \ \left(\frac{L}{W} G \right) = 0.212$$

$$MGT2{:} \frac{W}{L} = 1 \ \text{ and } \ \left(\frac{L}{W} G \right) = 0.409$$

$$\text{MGT3:} \frac{W}{L} = 0.5 \text{ and } \left(\frac{L}{W}G\right) = 0.576$$

It is noticed that the $SNR(f)$ is maximum for $W/L = 0.5$, and for smaller values of this ratio. For the same B magnetic induction, increasing the channel, $SNR(f)$ decreases with 44% width for $W=2L$ As compared to the $W/L = 0.5$ structure.

In case of $1/f$ noise, by substituting (1.10) and (2.2) into (2.7) it is obtained:

$$SNR(f) \cong \frac{(ndLW_E)^{1/2}}{2\alpha^{1/2}} \cdot \mu_{H_n} \left(\frac{f}{\Delta f}\right)^{1/2} \cdot \left(\frac{L}{W_E}G\right) \cdot B_\perp \qquad (2.9)$$
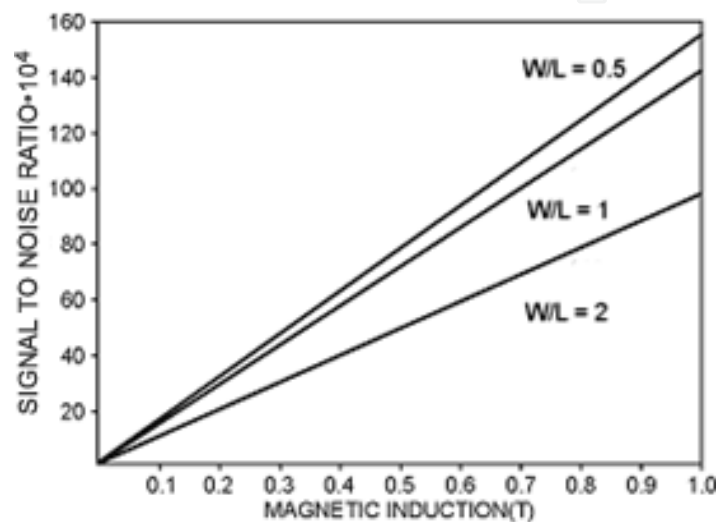
Fig. 2.7. SNR(f) depending on B for three devicesof different geometry.

To illustrate the $SNR(f)$ dependence on device geometry three split-drain magnetotransistor structures realised on Si were simulated (figure 2.8).
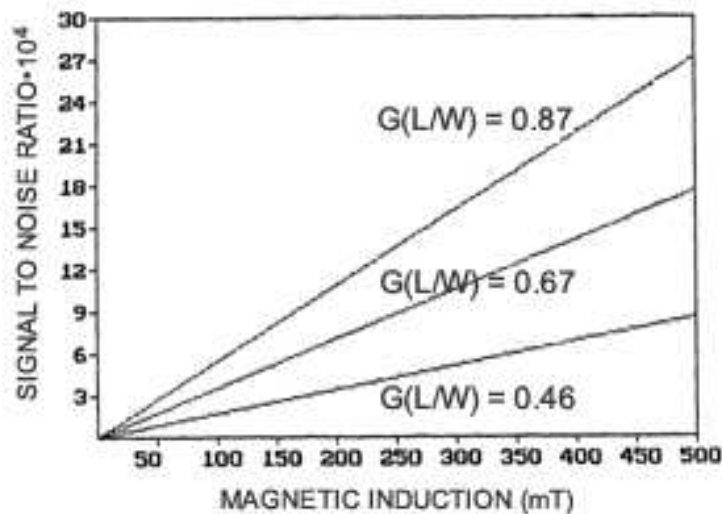
Fig. 2.8. $SNR(f)$ depending on B for three devices of different geometry.

$$G(L/W) = 0.46$$

$$MGT2 : W = 50\mu m , \; L = 50\mu m ,$$

$$G(L/W) = 0.67$$

$$MGT3; W = 50\mu m , \; L = 100\mu m ,$$

It is considered that: $f = 4Hz$, $\Delta f = 1Hz$, $n = 4.5 \cdot 10^{15} cm^{-3}$, $\alpha = 10^{-7}$, $\delta = 0.5\mu m$, $q = 1.9 \cdot 10^{-6} C$ the devices being biased in the linear region and the magnetic field having a low level.

For the same magnetic induction B, $SNR(f)$ is maximum in case of $L = 2W_E$. The increasing of the canal length causes the decreasing of $SNR(f)$ with 35.2% for a square structure and with 69.1% for $W = 2L$. In figure 2.9 is presented the dependence of SNR on B for three magnetotransistors whit the same geometry $W/L = 0,5$, $L = 200 \; \mu m$ realised from different:
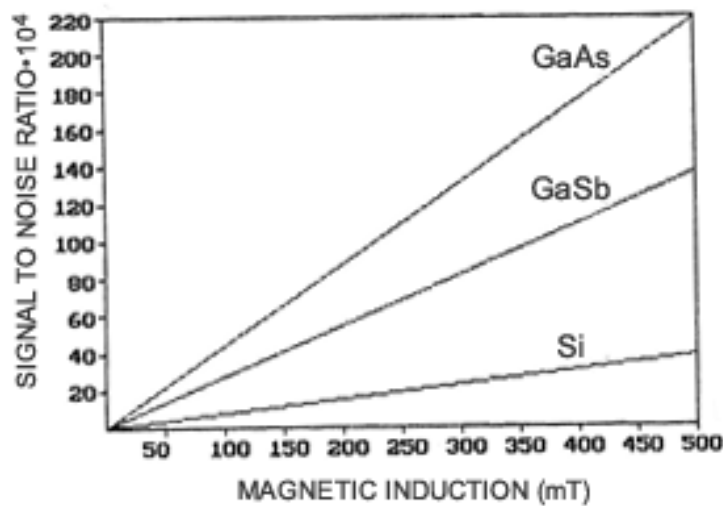
Fig. 2.9. $SNR(f)$ depending on B for three devices of different materials

$$MDD1(\text{Si}, \; \mu_{HCh} = 0,07 \; m^2 V^{-1} s^{-1}),$$

$$MDD2(\text{GaSb}, \mu_{HCh} = 0,25 \; m^2 V^{-1} s^{-1}),$$

$$MDD3(\text{GaAs}, \; \mu_{HCh} = 0,42 \; m^2 V^{-1} s^{-1}),$$

A high value of carrier mobility cause the increasing of SNR So for $B = 0.5T, SNR(f)$ increase with 65% for $GaAs$ comparative $GaSb$

2.5 The detection limit of sensor in mos technology

A convenient way of describing the noise properties of a sensor is in terms of detection limit, defined as the value of the measurand corresponding to a unitary signal-to-noise ratio.

In case of shot noise, for double-drain magnetotransistors using (2.8) it results for detection limit:

$$B_{DL} \leq \frac{2\sqrt{2}\left(q\Delta f\right)^{1/2}}{\mu_{HCh}\left(L/W\right)G} I_D^{-1/2} \qquad (2.10)$$

To illustrate the B_{DL} dependence on device geometry (figure 2.10) three double-drain magnetotransistors structures on silicon $\mu_{HCh} = 0.07 m^2 V^{-1} s^{-1}$ were simulated and having different ratios $\left(W = 100\mu m\right)$.

$$MGT1:\ W/L = 0.5\ ;$$

$$MGT2:\ W/L = 1\ ;$$

$$MGT3:\ W/L = 2$$

It is noticed that the B_{DL} is minimum for $W/L = 0.5$ structure. For optimal structure B_{DL} decreases at materials of high carriers' mobility.

In figure 2.11 the material influence on B_{DL} values for three double-drain magnetotransistor structures realised from *Si*, *GaSb* and *GaAs* can be seen having the same size: $L = 200\mu m$, $W = 100\mu m$.

$$MGT1:\ Si \text{ with } \mu_{HCh} = 0.07 m^2 V^{-1} s^{-1}\ ;$$

$$MGT2:\ GaSb \text{ with } \mu_{HCh} = 0.25 m^2 V^{-1} s^{-1}\ ;$$

$$MGT3:\ GaAs \text{ with } \mu_{HCh} = 0.42 m^2 V^{-1} s^{-1}\ .$$

By comparing the results for the two types of Hall devices used as magnetic sensors it is recorded a lower detection limit of almost 2-order in double-drain magnetotransistors. A high value of carrier mobility causes the increasing of *SNR(f)*. So for $B = 0,5T$, *SNR(f)* increase with 60% for GaAs comparative with GaSb.
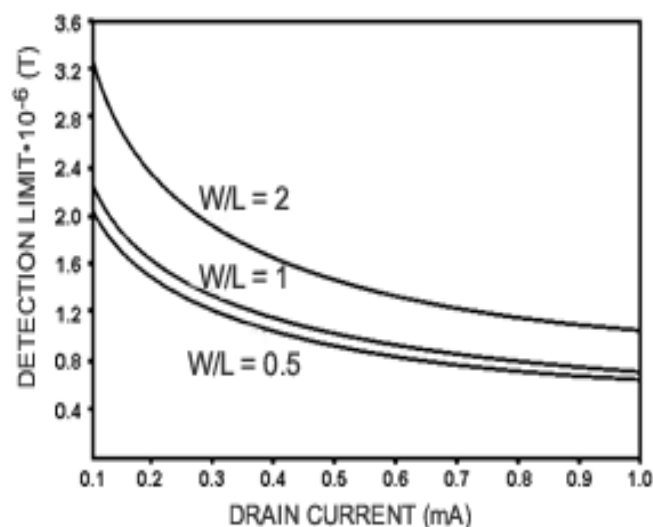
Fig. 2.10. B_{DL} depending on the drain-current for three devices of different geometry.
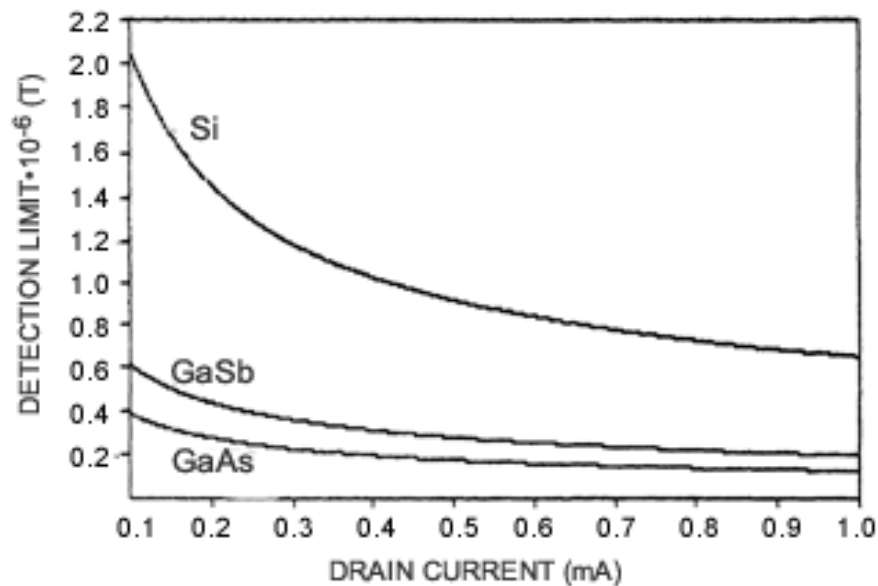
Fig. 2.11. B_{DL} depending on the drain current for three device of different materials.

2.6 The nemi for double-drain magnetotransistors

The noise current at the output of a magnetotransistors can be interpreted as a result of an equivalent magnetic induction.The mean square value of noise magnetic induction (*NEMI*) is defined by [8]:

$$\left\langle B_N^2 \right\rangle = \frac{\int_{f1}^{f2} S_{NI}(f) \cdot df}{\left(S_I \cdot I_D\right)^2} \tag{2.11}$$

Here S_{NI} is the noise current spectral density in the drain current, and (f_1, f_2) is the frequency range.

In case of shot noise, in a narrow frequency band around the frequency f by substituting (1.8) and (2.3) into (2.11) it results:

$$\left\langle B_N^2 \right\rangle = 2Iq\Delta f \cdot 4 \cdot \left(\frac{W}{L}\right)^2 \frac{1}{G^2 \mu_{HCh}^2} \cdot \frac{1}{I_D^2} \le 8q\left(\frac{W}{L}\right)^2 \cdot \frac{\Delta f}{G^2} \cdot \frac{1}{\mu_{HCh}^2} \cdot \frac{1}{I_D} \tag{2.12}$$

Considering the condition of low value magnetic field fulfilled $\left(\mu_H^2 B^2 << 1\right)$, it is obtained a maximum value for $\frac{L}{W}G = 0,74$, if $\frac{W}{L} < 0,5$ [5]. In this case:

$$\left\langle B_N^2 \right\rangle_{\min} \le 14,6q(\Delta f / I_D)\mu_{HCh}^{-2} \tag{2.13}$$

To emphasize the dependence of *NEMI* on device geometry there were simulated (figure 2. 12) three double-drain magnetotransistors structures realised on silicon, $\mu_{HCh} = 0,07 m^2 V^{-1} s^{-1}$, and having different ratios W / L ($W = 50\mu m$). The devices were based in the linear region and magnetic field has a low level $\left(\mu_H^2 B^2 << 1\right)$.

MGT1: $W / L = 0.5$ and $(L / W)G = 0.56$

$$\text{MGT2: } W/L = 1 \text{ and } (L/W)G = 0.409$$

$$\text{MGT2: } W/L = 2 \text{ and } (L/W)G = 0.212$$

It is noticed that the *NEMI* is minimum for $W/L = 0.5$, and for smaller values of this ratio. The decreasing of the channel length causes the increasing of $NEMI(f)$ with 40,8% for a square structure $W = L$, and with 173% for $W = 2L$.

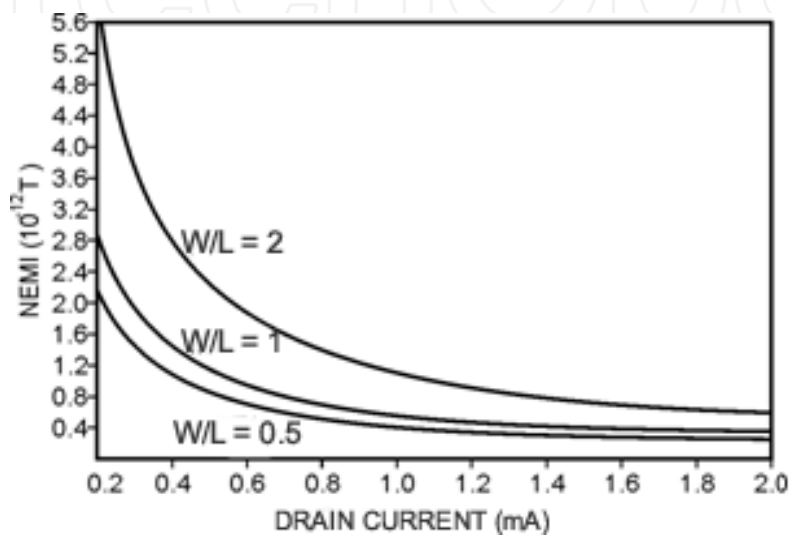In figure 2.13 NEMI values are shown obtained by simulation of three double-drain MOS magnetotransistors structures from different materials.

Fig. 2.12. The NEMI depending on the drain current for three devices of different geometry
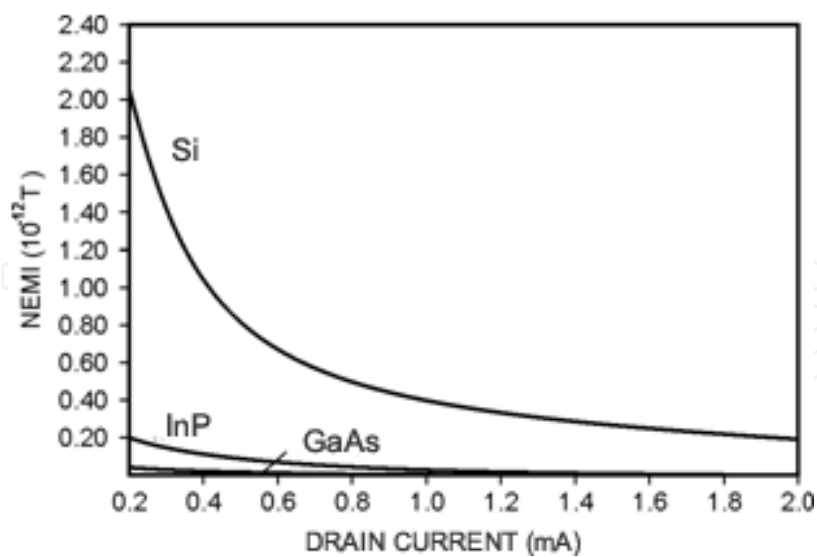
Fig. 2.13. The NEMI depending on drain current, for threedevices of different materials.

$$\text{MGT1: } Si, \ \mu_{HCh} = 0.07 \, m^2 V^{-1} s^{-1}$$

$$\text{MGT2: } InP, \ \mu_{HCh} = 0.23 m^2 V^{-1} s^{-1} \ ;$$

$$MGT3{:}GaAs,\ \mu_{HCh} = 0.42m^2V^{-1}s^{-1}$$

2.7 The $S_{NB}(f)$ for double- drain mosfet

From (2.11) it is obtained the noise-equivalent magnetic induction spectral density:

$$S_{NB}(f) = \frac{\partial < B_N^2 >}{\partial f} = \frac{S_{NI}(f)}{S_A^2} \tag{2.14}$$

In case of shot noise, by analogy with (2.12) it results that:

$$S_{NB}(f) = 2qI \cdot 4\left(\frac{W}{L}\right)^2 \cdot \frac{1}{G^2\mu_{HCh}^2} \cdot \frac{1}{I_D^2} \leq 8q\left(\frac{W}{L}\right)^2 \cdot \frac{1}{G^2} \cdot \frac{1}{\mu_{HCh}^2} \cdot \frac{1}{I_D} \tag{2.15}$$

Conclusions

Although magnetotransistors have a low magnetic sensitivity, very large signal-to-noise ratios are obtained, hence, a high magnetic induction resolution is resulting. A signal-to-noise ratio of about $8 \cdot 10^5$ at a magnetic induction of *200mT* has been obtained at double-drain magnetotransistors in case *GaAs*.

The analysis of the characteristics of magnetotreansistors structures shows that the $W/L = 0.5$ ratio is theoretically favourable to high performance regarding the noise-equivalent magnetic induction.

The noise equivalent magnetic induction lowers with the increase of carriers mobility, this increase being significant for drain currents of relatively low values.

From double-drain MOSFET magnetotransistors, in case of shot noise, the $W/L = 0.5$ structure provides superior *SNR* values, and smaller detection limit values. A detection limit of about $0,2 \cdot 10^{-6}T$ at a total drain-current of *0,5 mA* has been obtained at double-drain MOSFET magnetotransistor in case *GaAs*.

Also substituting the silicon technology by using other materials such as *GaAs* or *InSb* with high carriers mobility enables to manufacture higher characteristics devices.

2.8 The measurement of the torque at the naval engine shaft

Efficient operation of maritime ships and prevention of some considerable damages require supervision, measurement and adjusting of the main engine parameters together with other equipment and installations on board ship. Of a great importance is the permanent knowledge of the torque developed at the naval main engine shaft. The measurement of the mechanic torque M can be made based on the twisting angle Ψ that appears between two transversal sections of the shaft when this transmits mechanical power.

Following this purpose two disks S1, S2 are placed within those two sections which contain along their circumference, magnetic recording of two sinusoidal signals or rectangular of equal frequency.

Two transducers made with Hall magnetic microsensors positioned in the immediate vicinity of those two disks, allow during the rotation of the shaft to furnish information regarding the phase difference between those two signals, the rotation of the shaft to furnish

information regarding the phase difference between those two signals, owing to its torque. The result of the measurement is exposed in numerical form.

2.8.1 Transducer based on the double-drain

Figure 2.15 shows the electrical diagram of a transducer based on double-drain magnetotransistors.

If the double-drain MOSFET works in saturation the differential output voltage is the following :

$$\Delta V_D = \mu_{HCh} \frac{L}{W} G V_R B_\perp \tag{2.16}$$

This voltage is applied to a comparator with hysteresis, which acts as a commutator. The existence of the two travel thresholds ensure the immunity at noise to the circuit. The monostable made with *MMC 4093* ensures the same duration for the transducers generated pulses.
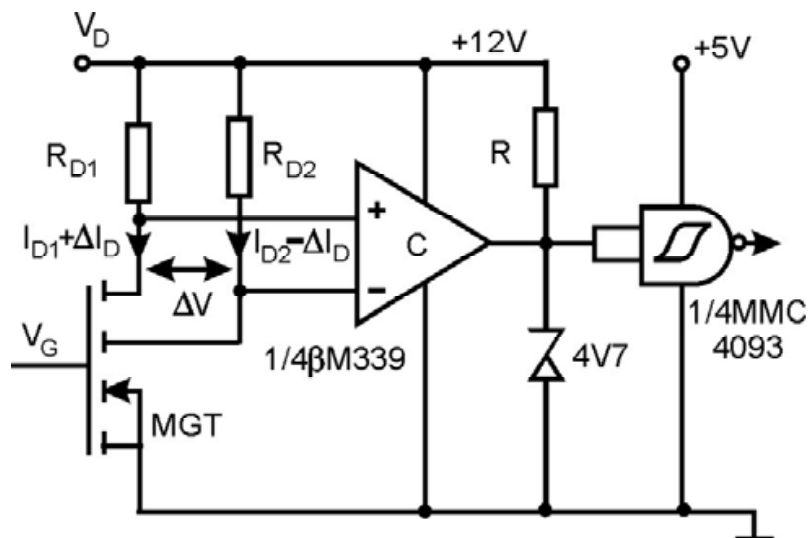
Fig. 2.15. The electrical diagram of transducer

2.8.2 Block diagram of the instalation and description of function

The disks with magnetical registration are distributed in such a way that the free rotation of the shaft, over the time when it is not transmitted the mechanical power, the signals produced by those two transducers are rigorously on phase.

At the power coupling, owing to the shaft torsion between those two sections S1 and S2 (figure 2.16) a twisting angle Ψ appears to which a phase difference between those two signals corresponds..

The work of installation may be supervised by means of the block diagram (figure 2.17) and by the forms of wave shown in figure 2.18.

The signals from the output of those two monostable CBM1, and CBM2 are applied to the differentiating circuits CD1 and CD2 which activate the bistable circuit CBB.

The positive impulses of the signal (b) put the flip-flop in the state 1 (high) and the positive impulses of the signal (b') bring it back to the state 0 (low).
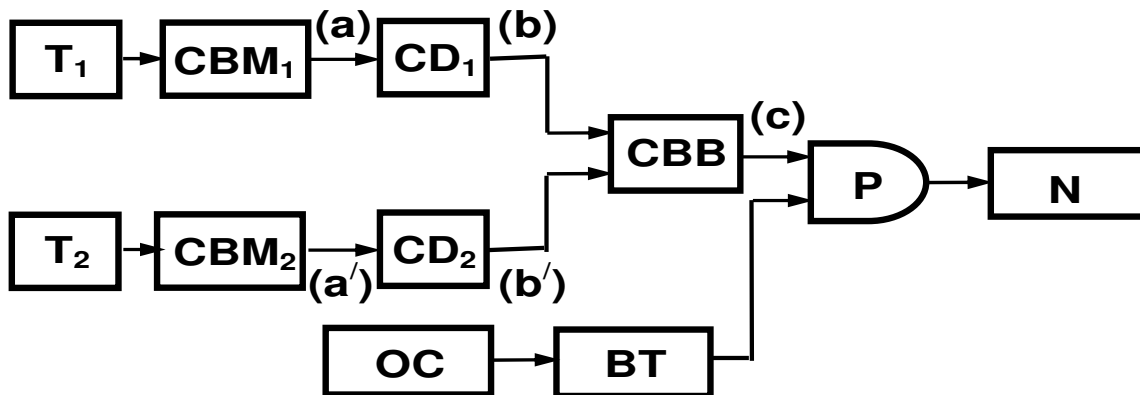
Fig. 2.17. Bloc diagram of the circuit for the measurement of mechanical torque
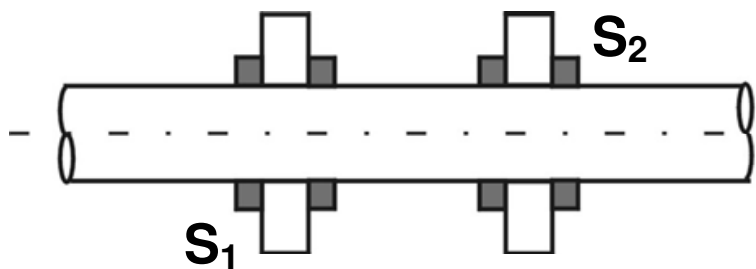

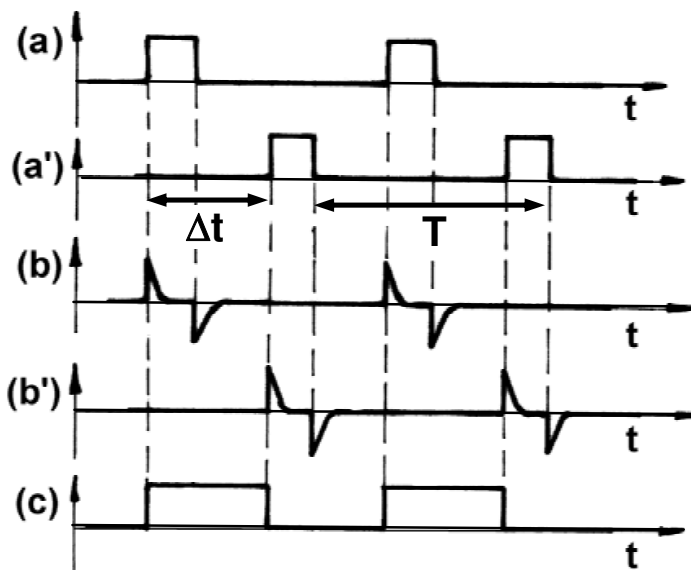Fig. 2.16. Disc distribution on ship's engine shaft

Fig. 2.18. Wave forms for the circuit measuring the torque

In this way at the output of flip-flop a right-angular signal (C) having the period T of magnetically registration and duration $\Delta t \sim \Psi$ is noticed description of the circuit gate P. The time interval Δt is measured by counting the signal periods of a quartz-oscillator, periods comprised within this interval.

Signal is applied to numerator N as long as gate P is open.

Numerator indications are modified at each impulse, so that the time interval between two states will be equal with the period of the given signal and it will represent the unit in which is expressed the result of measurement.

Remarks

In the case of very small value of the torsion twisting angle Ψ , the resolution capacity of the bi-state situation can be exceeded in which there are placed initially those two disks so as the transmitted signals by the traductors at free rotation of the shaft to be in opposition of phase.

Those two monostable circuits assure abrupt fronts to operational impulses of bi-stable resulting in the reduction of the level error of starting it.

The measurement precision depends on the relative error of numerator error of level starting of the bi-stable and the relative error of quartz oscillator.

3. The lateral bipolar magnetotransistor

3.1 General caracterisation of the lateral bipolar magnetotransistor

Figure 3.1 illustrates the cross section of a lateral bipolar magnetotransistor structure, operating on the current deflection principle, realized in MOS integrated circuits technology [8].

The n^+ regions of emitter E and primary collector C, are laterally separated on an L distance from base type p region. The two p^+ base contacts, allow for the application of the drift-aided field $\bar{E}_a$. On its action the most part of the minority carriers injected into the base drift to primary collector, producing collector current I_C . However some of electrons diffuse downwards to the n type substrate (the secondary collector) and thus produce the substrate parasitic current I_S .

In the presence a magnetic induction $B_\perp$, perpendicular to the plane of the section the ratio between I_C and I_S, change because of the current deflection.
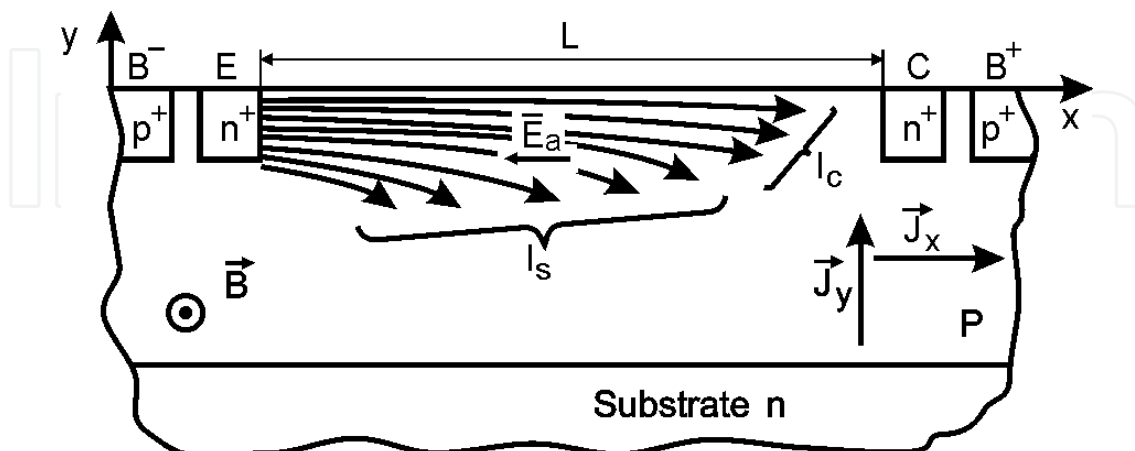

Fig. 3.1. Cross section of lateral magnetotransistor

In order to describe the qualitative operation of the device, let us assume that it is adequately biased for the forward active operation. If the very small magnetic field $\bar{E}_a$,is

oriented as shown in figure 3.1, the electrons are deviated to substrate junction. Only a few electrons will contribute to collector current.

The area from base region, between the emitter contact and collector contact, operates as a short Hall plate, and an induction field $\bar{B}$ causes the deflection of current lines. The transverse will be:

$$I_Y = J_Y (LW) \tag{3.1}$$

where W is the dimension along the axis Z.

In the absence of a induction $\bar{B}$, the current density along the axis X has the following expression:

$$J_X = \frac{I_C}{WY} \tag{3.2}$$

The Y parameter takes values in (y_{jn}, y_{jp}). Here y_{jn} and y_{jp} denote the junction depths of the collector region and the *p*-well respectively.

If it is considered the Hall angle expression $tg\theta_{Hn} = \mu_{Hn} \cdot B$ [6] then it is obtained:

$$J_Y = J_X \cdot tg\theta_{Hn} = \frac{(\mu_{Hn} B) I_C}{WY} \tag{3.3}$$

By substituting (3.3) into (3.1) it results:

$$I_H = I_Y = (L / Y) I_C \mu_{Hn} B_\perp = \Delta I_C \tag{3.4}$$

where μ_{Hn} is the Hall mobility of electrons in the base region.

3.2 The sensor response and the sensitivity

A magnetotransistor may be regarded as a modulation transducer that converts the magnetic induction signal into an electric current signal.

This current signal or output signal is the variation of collector current, caused by induction $\bar{B}_\perp$.

The sensor response is expressed by:

$$h(B) = \frac{\Delta I_C}{I_C} = \frac{L}{Y} \mu_{Hn} \cdot B \tag{3.5}$$

and it is linear for induction values which satisfy the condition: $\mu_H^2 \cdot B_\perp^2 \ll 1$. In figure 3.1 the geometry influence on $h(\overline{B})$ values for three magnetotransistor structures can be seen. They are realized on silicon ($\mu_{Hn} = 0.15 m^2 V^{-1} s^{-1}$) and have different ratios L/Y ($L = 50 \mu m$).

$$\text{MGT}_1 : \frac{L}{Y} = 0,5 ;$$

$$\text{MGT}_2: \frac{L}{Y} = 1 \; ;$$

$$\text{MGT}_3: \frac{L}{Y} = 2 \; ;$$

For the same geometry ($L/Y = 0.5$) the sensor response depends on material features. In figure 3.2 $h(\overline{B})$ values for two sensor structures realized on Si ($\mu_{Hn} = 0.15 m^2 V^{-1} s^{-1}$) and GaAs ($\mu_{Hn} = 0.80 m^2 V^{-1} s^{-1}$)are shown .
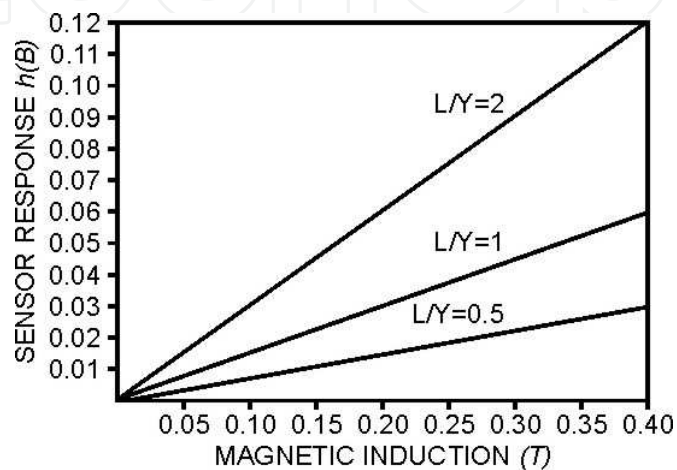

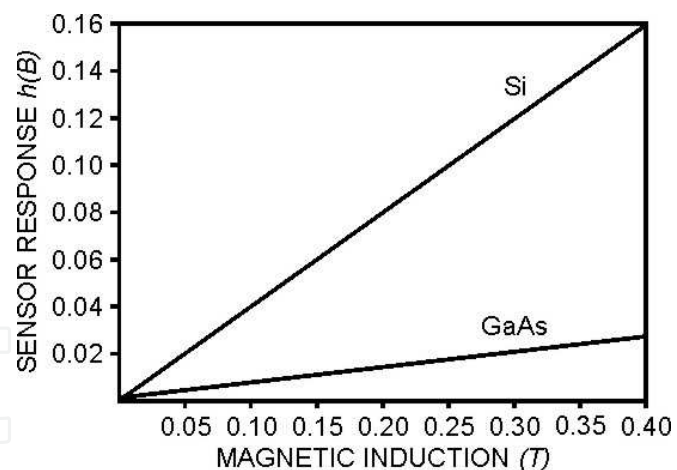Fig. 3.2. The $h(B)$ depending on B for three devices of different geometry

Fig. 3.3. The $h(B)$ on B on the two sensors of different materials

We can see that the sensors made of high mobility materials have superior response. For the same magnetic induction $B = 0.2T$ at the GaAs device, $h(\overline{B})$ increases 5.6 times compared to that value for the silicon.

The magnetic sensitivity related to the devices current is defined as follows:

$$S_I = \frac{1}{I_C} \left| \frac{\Delta I_C}{B} \right| = \frac{L}{Y} |\mu_{Hn}| \tag{3.6}$$

For a given induction $(B = 0.4T)$ and at given collector current $I_C = 1mA$, the sensitivity depends of the device geometry and the material properties. In table 3.1 are presented the obtained values for five magnetotransistors structures.

MGT	L/Y	μ_{Hn} $(m^2V^{-1}s^{-1})$	$S_1(T^{-1})$
MGT$_1$ (Si)	3	0.15	0.45
MGT$_2$ (Si)	1	0.15	0.15
MGT$_3$ (Si)	0.5	0.15	0.075
MGT$_4$ (GaAs)	3	0.80	2.40
MGT$_5$ (GaSb)	3	0.50	1.50

Table 3.1 The numerical values of the supply-current related sensitivity

3.3 The offset equivalent magnetic induction

For bipolar lateral magnetotransistor presented in figure 4 the offset current consists in the flow of minority carriers which, injected into the base region in absence of magnetic field diffuse downwards and are collected by the secondary collector S.

The main causes of the offset are due to the misalignment of contacts to non-uniformity of the thickness and of the epitaxial layer doping. Also a mechanical stress combined with the piezo-effect, may produce offset.

To describe the error due to the offset to describe the error due to the offset the magnetic induction is determined, which is determined the magnetic induction, which produces the imbalance $\Delta I_C = \Delta I_{Coff}$. The offset equivalent magnetic induction is expressed by considering the relation (3.6):

$$B_{off} = \frac{\Delta I_{Coff}}{S_I I_C} = \frac{1}{\mu_{Hn}} \cdot \frac{\Delta I_{Coff}}{I_C} \qquad (3.7)$$
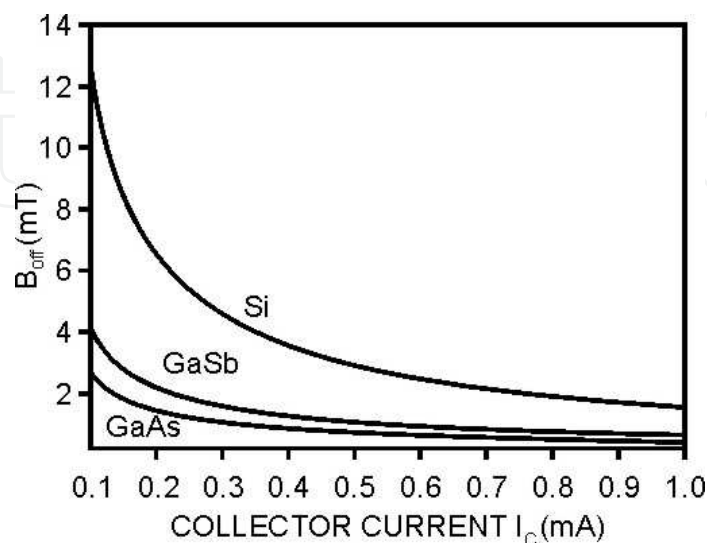
Fig. 3.4. The B_{off} depending on the I_C for three devices of different materials

Considering $\Delta I_{Coff} = 0.10\mu A$ and assuming that the low magnetic field condition is achieved, in figure 3.4 the dependence of B_{off} on I_c for three magnetotransistors is presented with the same geometry $L/Y = 0.5$ is presented, realized from different materials:

$$\text{MGT1: Si with } \mu_{Hn} = 0.15 m^2 V^{-1} s^{-1} ;$$

$$\text{MGT2: GaSb with } \mu_{Hn} = 0.50 m^2 V^{-1} s^{-1} ;$$

$$\text{MGT3: GaAs with } \mu_{Hn} = 0.85 m^2 V^{-1} s^{-1} ;$$

The offset-equivalent magnetic induction lowers with the increase of carriers' mobility.
So for the same collector current *Ic=0.1mA* the B_{off} value of the GaAs device decreases by 70% as compared to that of the silicon device.

3.4 Signal-to-noise ratio

The noise affecting the collector current of a magnetotransistors is shot noise and $1/f$ noise.
In case of *1/f* noise, and analogue with 1.11 it results:

$$SNR(f) \cong \frac{(nLYd)^{1/2}}{\alpha^{1/2}} \cdot \mu_{Hn} \left(\frac{f}{\Delta f} \right)^{1/2} \cdot \frac{L}{Y} B_\perp \tag{3.8}$$

To illustrate the $SNR(f)$ dependence on device geometry three lateral magnetotransistor structures realised on silicon were simulated (figure 3.5).

$$MGT_1 : L/Y = 0.5 ;$$

$$MGT_2 : L/Y = 1 ;$$

$$MGT_3 : L/Y = 4 .$$

It is considered that $f = 1.5 Hz$, $\Delta f = 1 Hz$, $\alpha = 10^{-7}$, $n = 4.5 \cdot 10^{21} m^{-3}$, $d = 10^{-5} m$ $q = 1.6 \cdot 10^{-19} C$ the device being biased in the linear region and the magnetic field having a low level.
For the same magnetic induction $B = 0,2T$ $SNR(f)$ is maximum in case $L = 4Y$. The increasing of the geometrical parameter Y causes the decreasing of *SNT(f)* with 50% for a square structure $Y = L$ and with 63.3% for $Y = 2L$.

In figure 3.6 it can be seen the material influence on *SNR(f)* values for three sensors MGT_1, MGT_2, MGT_3 realised on Si ($\mu_{Hn} = 0.15 m^2 V^{-1} s^{-1}$, $f = 1.2 Hz$), GaSb ($\mu_{Hn} = 0.50 m^2 V^{-1} s^{-1}$, $f = 5 Hz$) and GaAs ($\mu_{Hn} = 0.80 m^2 V^{-1} s^{-1}$, $f = 7.8 Hz$); $L = 3Y$, $Y = 20\mu m$.
In case of shot noise (see equation1.8) is obtained:

$$SNR(f) = \frac{1}{\sqrt{2}} \mu_{Hn} \frac{L}{Y} \cdot \frac{I_C}{(q \cdot I \cdot \Delta f)^{\frac{1}{2}}} \cdot B_\perp \leq 0.707 \mu_{Hn} \frac{L}{Y} \left(\frac{I_C}{q \Delta f} \right)^{1/2} \cdot B_\perp \tag{3.9}$$
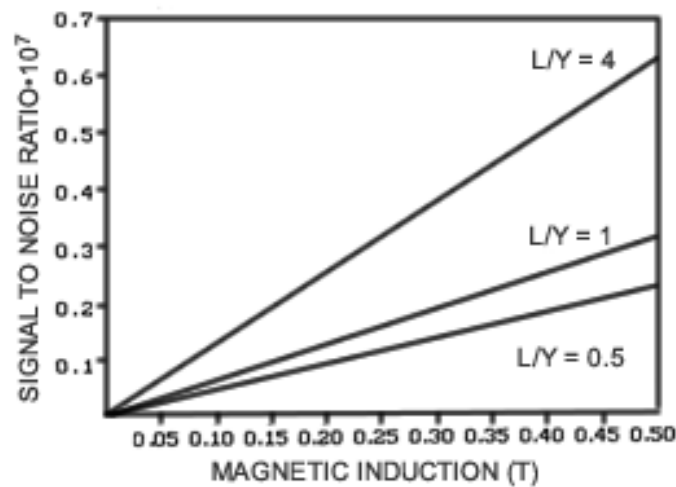
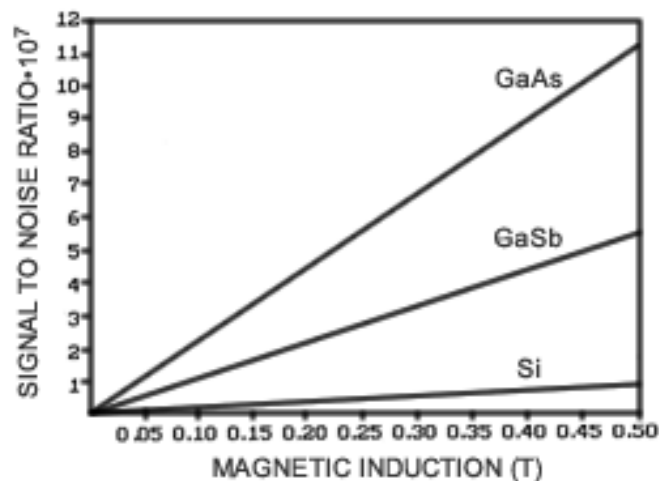Fig. 3.5. *SNR(f)* depending on magnetic induction for three devices of different geometry

Fig. 3.6. SNR(f) depending on collector current for three devices of different materials

In figure 3.7 is shown the $SNR(f)$ dependence in collector current of three magnetotransistor structures of different materials ($L/Y = 5, \Delta f = 1 Hz, B = 0.2T$)

$$MGT_1: \text{Si with } \mu_{Hn} = 0.15 m^2 V^{-1} s^{-1}$$

$$MGT_2: \text{Ga Sb with } \mu_{Hn} = 0.50 m^2 V^{-1} s^{-1}$$

$$MGT_3: \text{Ga As with } \mu_{Hn} = 0.80 m^2 V^{-1} s^{-1}$$

A high value of carrier mobility causes the increasing of $SNR(f)$. So for $I_c = 0.2 mA$, $SNR(f)$ increases with 60% for Ga As comparative with GaSb.

To emphasise the dependence of $SNF(f)$ on device geometry there (figure 3.8) three magnetotransistor structures realised on silicon ($\mu_{Hn} = 0.15 m^2 V^{-1} s^{-1}$) were simulated having different ratios.

$$L/Y \ (L = 50 \, \mu m; B = 0.2T;) \ \Delta f = 1 Hz$$

$$MGT_1 : L/Y = 5$$

$$MGT_2 : L/Y = 3$$

$$MGT_3 : L/Y = 2$$
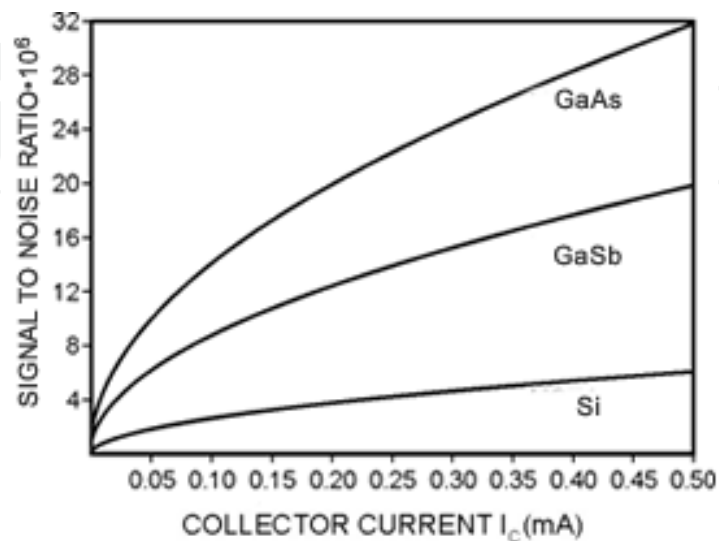
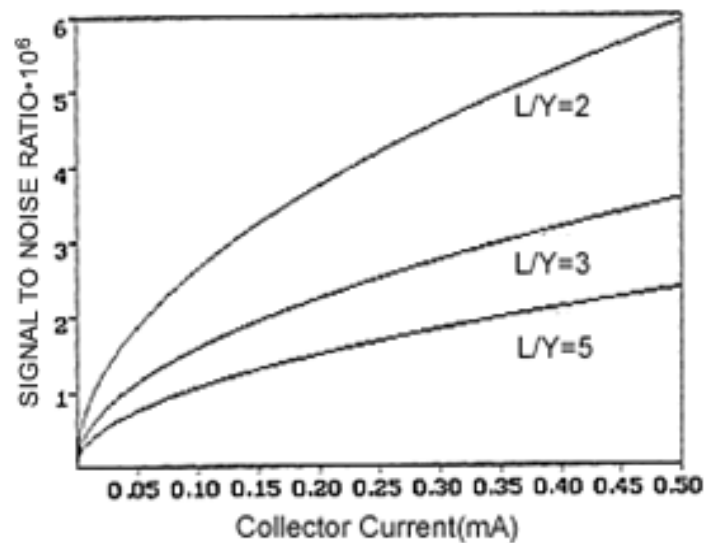Fig. 3.7. SNR(f) depending on collector current for three devices of different materials

Fig. 3.8. SNR(f) depending on I_C for three devices of different geometry

3.5 The detection limit

A convenient way of describing the noise properties of a sensor is in terms of detection limit, defined as the value of the measured corresponding to a signal-to-noise ration of one. In case of shot noise, it is obtained from expression (3.9):

$$B_{DL} \geq \frac{(2q\Delta f)^{1/2}}{\mu_{Hn}} \cdot \frac{Y}{L} \cdot I_C^{-1/2} \tag{3.10}$$

In figure 3.9 are shown B_{DL} values obtained for three magnetotransistor structures made of different materials:

$$MGT_1: \text{ Si } (\mu_{Hn} = 0.15 m^2 V^{-1} s^{-1}),$$

$$MGT_2 : \text{GaSb } (\mu_{Hn} = 0.50 m^2 V^{-1} s^{-1})$$

$$MGT_3 : \text{GaAs } \mu_{Hn} = 0.80 m^2 V^{-1} s^{-1}).$$

A high value carrier's mobility causes the decreasing of detection limit so B_{DL} decreases with 45% for *GaAs* comparative with *GaSb*.
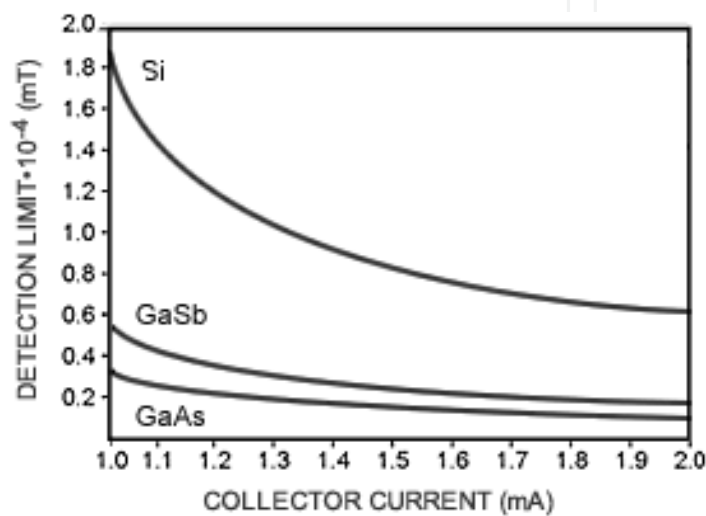

Fig. 3.9. B_{DL} depending on collector current for three devices of different materials

3.6 The noise equivalent magnetic induction

The noise current at the output of a magnetotransistor can be interpreted as a result of an equivalent magnetic induction. The mean square value of noise equivalent magnetic induction (NEMI) is defined by:

$$\left\langle B_N^2 \right\rangle = \frac{\int_{f1}^{f2} S_{NI}(f) \cdot df}{(S_I \cdot I_C)^2} \tag{3.11}$$

Here S_{NI} is the noise current spectral density in the collector current, and (f_1, f_2) is the frequency range.

In case of shot noise, the mean square value of noise equivalent magnetic induction (NEMI) is defined by similarity with relation (1.13):

$$\left\langle B_N^2 \right\rangle \le 2q \left(\frac{Y}{L} \right)^2 \frac{\Delta f}{\mu_{Hn}^2} \cdot \frac{1}{I_C} \tag{3.12}$$

In figure 3.10 NEMI values for three magnetotransistor structures made of different materials ($Y / L = 0.5; \Delta f = 1 Hz$) are shown MGT_1: Si with $\mu_{Hn} = 0.15 m^2 V^{-1} s^{-1}$

$$MGT_2: \text{Ga Sb with } \mu_{Hn} = 0.50 m^2 V^{-1} s^{-1}$$

$$MGT_3: \text{Ga As with } \mu_{Hn} = 0.85 m^2 V^{-1} s^{-1}$$

For the same collector current $I_c = 0,2mA$ the NEMI value of the Ga As device decreases by 25.6 times as compared to that of the silicon device.
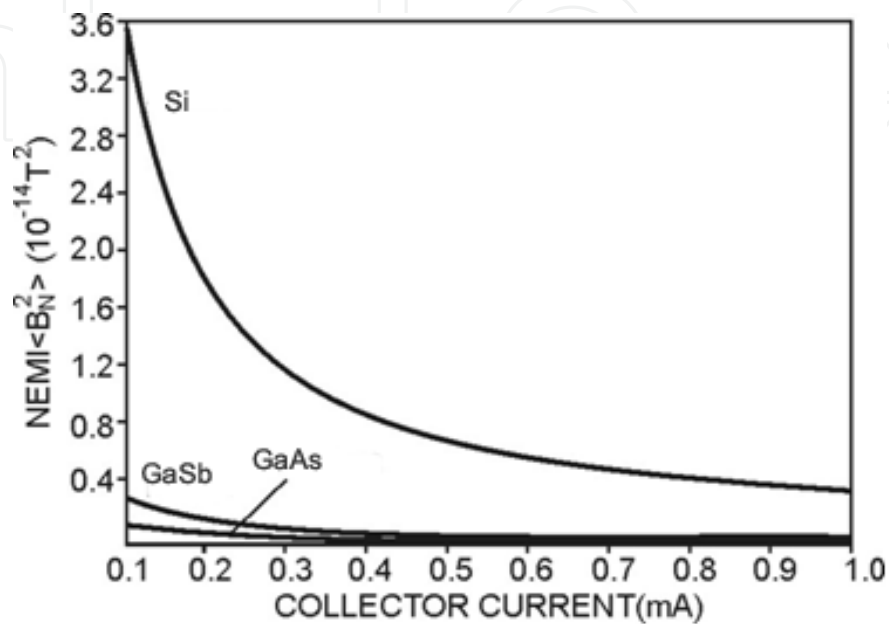

Fig. 3.10. NEMI depending on the collector current for three devices of different materials

To emphasise the dependence of NEMI device geometry, (figure 3.11) two magnetotransistor structures realised on silicon and having different ratios were simulated:
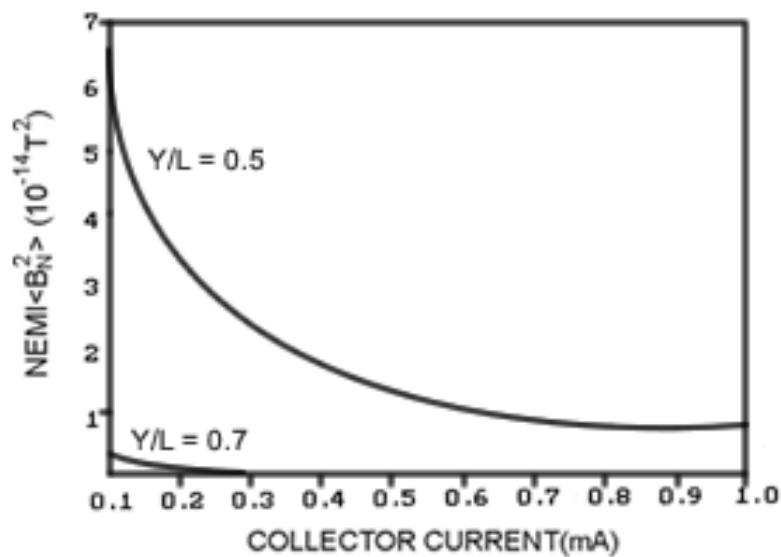
Fig. 3.11. NEMI depending on the collector current for two devices of different geometry

$$Y/L \quad (L = 50 \mu m,$$

$$MGT_1 : Y/L = 0.5 \; ;$$

$$MGT_2 : Y/L = 0.7 \;).$$

3.7 The noise-equivalent magnetic induction spectral density

From (3.11) the noise-equivalent magnetic induction spectral density is obtained:

$$S_{NB}(f) = \frac{\partial < B_N^2 >}{\partial f} = \frac{S_{NI}(f)}{S_A^2} \tag{3.13}$$

In a narrow frequency band around the frequency *f*, it results [8]:

$$S_{NB}(f) \le 2q \left(\frac{Y}{L} \right)^2 \frac{1}{\mu_{Hn}^2 I_C} \tag{3.14}$$

In figure 3.12 S_{NB} *(f)* values for three magnetotransistor structures made of different materials ($Y/L = 0.5 ; \Delta f = 1 Hz$) are shown

$.MGT_1$: Si, with $\mu_{Hn} = 0.15 m^2 V^{-1} s^{-1}$

MGT_2: Ga Sb, with $\mu_{Hn} = 0.50 m^2 V^{-1} s^{-1}$

MGT_3: Ga As, with $\mu_{Hn} = 0.80 m^2 V^{-1} s^{-1}$

The noise-equivalent magnetic induction spectral density lowers with the increase of carriers mobility, this increase being significant for collector currents of relatively low values. So for the collector current $I_C = 0.1 mA$, the offset equivalent magnetic induction value of the GaSb device decreases by 91.5% as compared to that of the silicon device
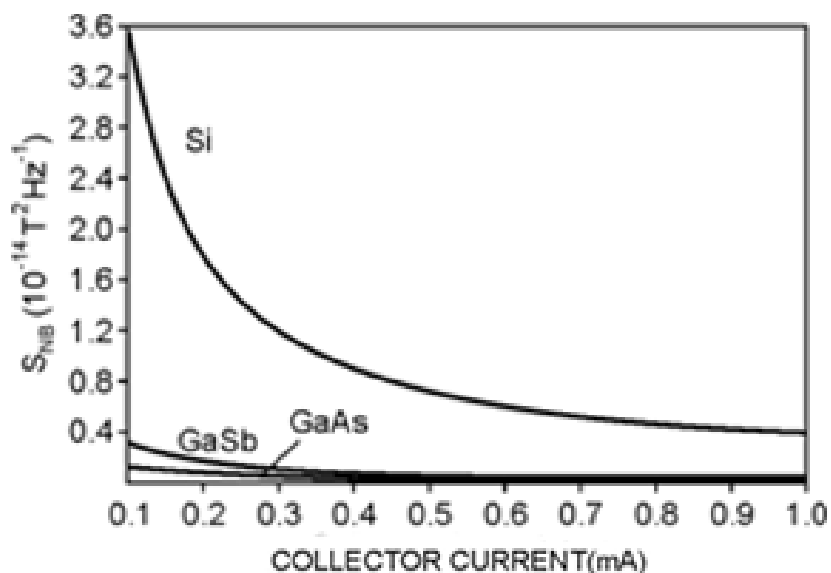

Fig. 3.12. The S$_{NB}$ (f) depending on the I_C for three devices of different materials

3.8 A system to maintain the horizontal position of certain naval equipment

The present paper proposes an original solution to increase the efficiency of cardanic suspension which ensures the stabilization of horizontal position for gyrocompass and radar antenna.

A. Two platforms that can spin simultaneously, but independent of each other, driven by two direct current reversible motors are used.
B. The signals that determine the value of the engine supply voltage are given by two position transducers made up of with lateral bipolar magnetotransistors in differential connection.

On merchant ships, the establishment of both the horizontal position of the gyroscopic compass and the radar antenna is accomplished with the help of the suspension on 3 gimbals circles which eliminates the unwanted effect of rolling and pitching for the values included in the range -10° ÷ 10°.

An original solution wherewith the system of the gimbals suspension becomes capable for the pitching angles of the ship that oversteps the mentioned limits is the use of 2 superimposed platforms which are simultaneously rotating, but independently.

The driving shaft which constitutes at the same time the sustaining element of the first platform is horizontally disposed and parallel with the longitudinal axis of the ship. It is supported by bearings whose bolsters are mounted on a fixed element in the ship's structure. By rotating it this platform decreases the effect of the rolling.

The second platform which holds the suspension gimbals system is also sustained by her own shaft whose bearings have the holders jammed tight on the first platform. Being on the longitudinal axis of the ship, the leading shaft of this platform enables a rotating motion which decreases the effect of the pitch. Each platform is operated by a reversible direct current motor.

The signals which determine the bridge driving voltage polarity for the 2 engines are given by the position transducers made with magnetic transistors in differential connection.

3.9 The presentation of the Hall transducer

The magnetotransistor used in the construction of the displacement transducer (figure 3.13) has the structure of a MOS transistor with long channel but operates as a lateral bipolar transistor with a drift-aided field in the base region.

In the presence of a magnetic field adequately oriented the collector current is very small. If the magnetic induction decreases the device current increase which brings about the collector potential variation ΔV_c :

$$\Delta V_C = R_{C1} \cdot \Delta I_C = R_{C1} \frac{L}{Y} \mu_{Hn} I_C B \tag{3.15}$$

The outlet of the magnetic transistor is connected to the inlet of a logical gate of „trigger Schmitt" type (ex.CDB413 or MMC4093) so that it supplies logic level „0" signal, when the magnetic induction increases and logic level „1" when the magnetic induction decreases.

The description of the position transducer

Because by rotating one of the platforms eliminates the effect of rolling, and the other one the effect of pitching we use a transducer for every platform. The two sensors of the transducer (figure 3.14) are magnetic transistors with MOS structure that function as lateral

bipolar transistors with supplementary drift field in the base region. For this kind of polarized device, the theoretical analysis shows that in case of a constant polarization, for a certain material and a geometry given to the device $\Delta I_c \approx B$. The two magnetic transistors are within the field of an magnetic pendulum. In the absence of the rolling or pitching, the pendulum is in a median position and the magnetic fields for the two magnetic transistors are equal. Therefore, $I_{C1} = I_{C2}$ and at the outlet of the transducer the voltage is $\Delta V_C = 0$.

At the inclination of the ship because of the rolling, to the port (or starboard) the induction value for a sensor is increasing, for exempt. MGT1, and decreasing for the other one. The balance of the two collector currents disappears even if $I_{C1} > I_{C2}$ the voltage at the outlet of the transducer is:

$$\Delta V_C = R_C(I_{C1} - I_{C2}) > 0 \qquad (3.16)$$

If the ship is listed in the other way, then $I_{C1} < I_{C2}$ and it results:

$$\Delta V_C = R_C(I_{C1} - I_{C2}) < 0 \qquad (3.17)$$

For the platform that can spin around an axis parallel to the longitudinal axis, the transducer pendulum moves in a plane perpendicular on the longitudinal axis of the ship, and for the other platform the magnetic pendulum of the transducer can move in a vertical plane in parallel with the longitudinal axis of the ship.
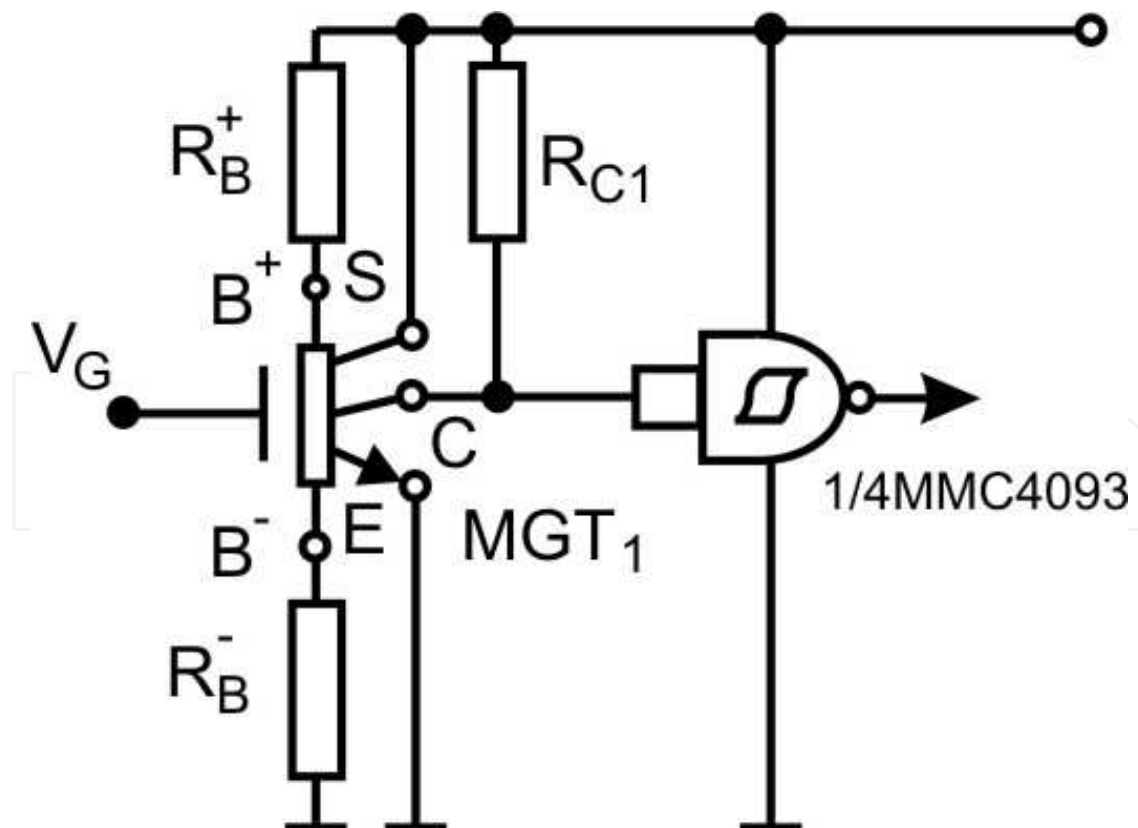

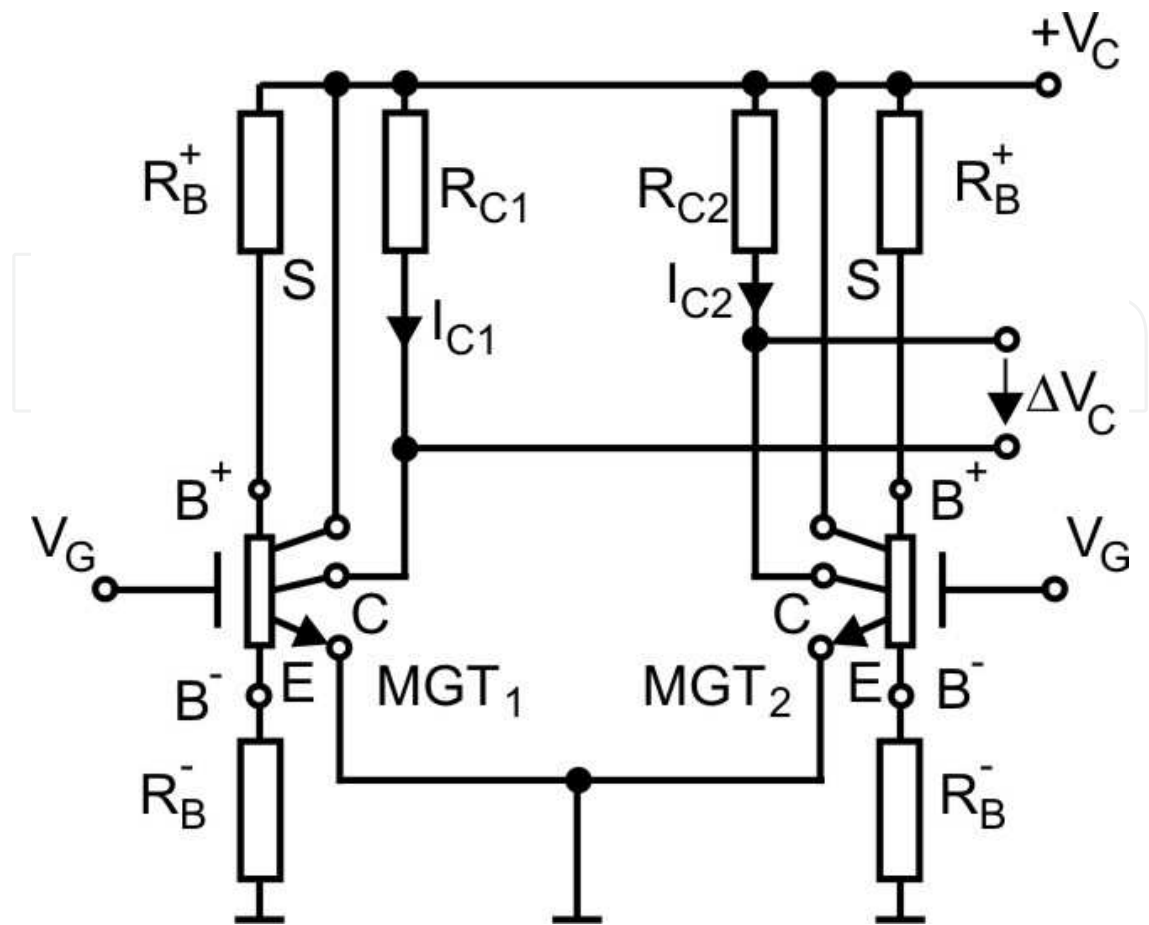Fig. 3.13. The electric diagram of Hall transducer

Fig. 3.14. The position transducer with magnetotransistor

Block diagram and the role of the component circuits

The block diagram (figure 3.15) contains: transducer T, integrator I, amplifier A, comparator C and the control assembly and energy supply of the motor BCA.

The level of signal to the outlet of the transducer is proportional to the ship's inclination angle, and its polarity shows the orientation of the ship's inclination.

The integrator eliminates the high frequency oscillations of the pendulum (the chip's oscillation frequency is reduced by fractions of *Hz*.

At the same time the integrator produces a small delay in the operating voltage variation of the engine, useful for the platform to reestablish the initial horizontal position. An essential contribution to this is the mechanic inertia of the system.

After amplification, the signal emitted by the transducer is compared with an additional reference transmission.

The comparator's threshold can be adjusted according to the delay produced by the integrator and the actuator mechanism inertia.
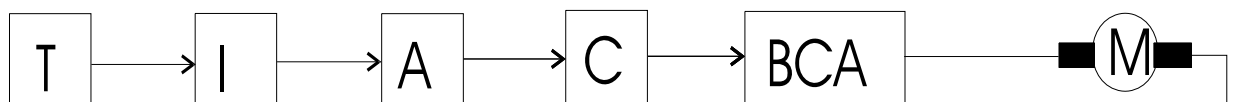

Fig. 3.15. The block diagram of the installation

The principle diagram and operating conditions

In figure 3.16 is presented the principle diagram of the transducer and amplifier. If the inclination of the ship to starboard brings the unbalance of the collector currents $I_{C_1} > I_{C_2}$ the transducer produces the signal:

$$\Delta V_C = R_C(I_{C_1} - I_{C_2}) = V_2 - V_1 > 0 \qquad (3.18)$$

The operational is in a differential amplifier configuration and the outlet voltage is:

$$V_0 = -(R_2 / R_1)\Delta V_C < 0 \qquad (3.19)$$

In figure 3.17 is presented the principle diagram of the motors' supply and control block.
When $V_0 < 0$ the voltage at the inputs of the two comparators have separate polarity. When $V_0 < 0$, $V_{i1} = V_0 - V_{r1} < 0$,and the output of the comparator C, is in DOWN state, therefore: $V_{01} = V_{0L} < 0$ which insures the blockage of the transistors T$_1$ and T$_3$.
In the same state , $V_0 < 0$ at the input of the comparator C$_2$ the voltage, is $V_{i2} = V_{r2} - V_0 > 0$, it passes in the UP state, $V_{02} = V_{0H} > 0$, which determines the conduction of the transistors T$_2$ and T$_4$, the polarity voltage at the jacks of the motor is the one indicated in the figure 3.17.
The direction of rotation is thereby given so that by moving the platform for the rolling compensation the balance of the two collector currents is re-established.
Clearly at the inclination of the ship to the port the outlet of the comparator C$_1$, passes in the UP state, conducts the transistors T$_1$, T$_3$ the direction of the bridge driving voltage changes and the motor will rotate in the opposite direction re-establishing the horizontal position of the platform.
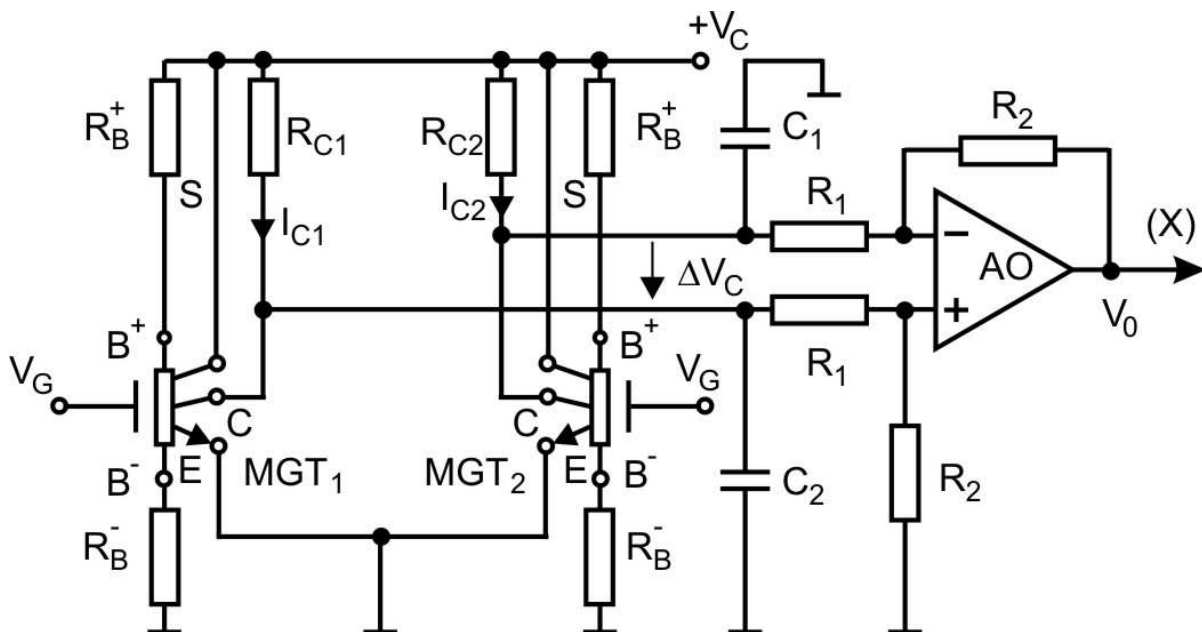

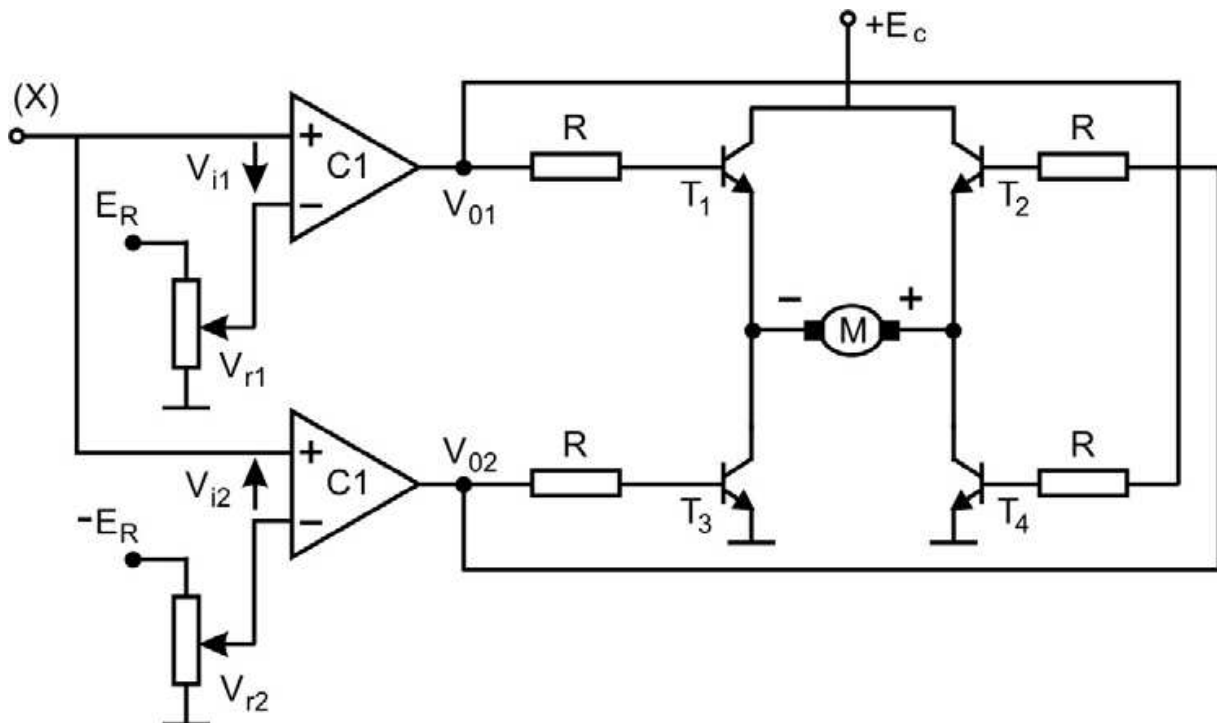Fig.3.16. The transducer and the differential amplifier

Fig. 3.17. The control and supply diagram of the motor

4. Conclusions

The presented system together with the cardanic suspension system eliminate the oscillation exceed of the ship in case of amplitudes that exceed $\pm 10^{\circ}$. The use of magnetotransistors as magnetic sensors allows for the achieving of same current-voltage conversion circuits, more efficient than the conventional circuits with Hall plates. Although the magnetotransistors have a low magnetic sensitivity, very large signal-to-noise ratios are obtained, hence, a high magnetic induction resolution is resulting. The possibility of having the sensor and the amplifier circuit on the same chip has lead to the achievement of transducers with high conversion efficiency as well as to increase in their range of practical work.

5. References

[1] Bodea M., "Traductoare integrate", Microelectronica, vol. 15, pp. 73-86, Editura Academiei R.S.Romania, Bucureşti, 1987

[2] Căruntu G., "Măsurări galvanomagnetice în dispozitive semiconductoare", Buletinul Sesiunii de Comunicări Ştiinţifice SECOMAR '99, Academia Navală "Mircea Cel Bătrân", Constanţa, vol. II, pp. 69-74, 1999

[3] Gray R.P., Meyer G.R., "Circuite integrate analogice. Analiză şi proiectare", Editura Tehnică, Bucureşti, 1973

[4] F.N. Hooge "1/f noise is no surface effect", Phys., 1969 Lett. 29A 139-40

[5] Middelhoek S., Audet S.A., "Physiscs of Silicon Sensors", Academic Press, London, 1989

[6] P.S. Kireev, "Fizica semiconductorilor", Editura Ştiinţifică şi Enciclopedică, Bucureşti 1977

[7] A. Nathan, H.P. Baltes, "Two dimensional numerical modelling of magnetic field sensors in CMOC technology", IEEE Trans Electron Devices ED-32 1212-19, 1985.

[8] R.S. Popovic , "Hall Effect Devices, Magnetic Sensors and Characterization of Semiconductors", Adam Hilger, Bristol , England , 1991
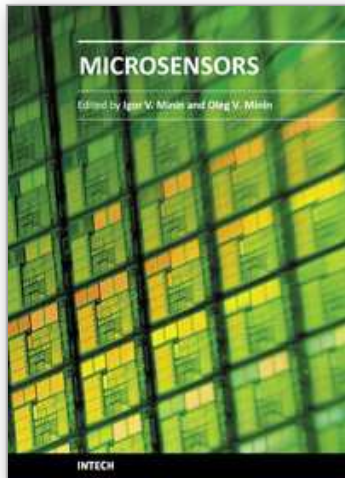
Microsensors

Edited by Prof. Igor Minin

This book is planned to publish with an objective to provide a state-of-art reference book in the area of microsensors for engineers, scientists, applied physicists and post-graduate students. Also the aim of the book is the continuous and timely dissemination of new and innovative research and developments in microsensors. This reference book is a collection of 13 chapters characterized in 4 parts: magnetic sensors, chemical, optical microsensors and applications. This book provides an overview of resonant magnetic field microsensors based on MEMS, optical microsensors, the main design and fabrication problems of miniature sensors of physical, chemical and biochemical microsensors, chemical microsensors with ordered nanostructures, surface-enhanced Raman scattering microsensors based on hybrid nanoparticles, etc. Several interesting applications area are also discusses in the book like MEMS gyroscopes for consumer and industrial applications, microsensors for non invasive imaging in experimental biology, a heat flux microsensor for direct measurements in plasma surface interactions and so on.

How to reference

In order to correctly reference this scholarly work, feel free to copy and paste the following:

INTECH
open science | open minds